ELSEVIER

Contents lists available at ScienceDirect

Gondwana Research

journal homepage: www.elsevier.com/locate/gr



Provenance analysis of Paleozoic strata in the Falkland/Malvinas Islands: Implications for paleogeography and Gondwanan reconstructions



J.R. Malone ^{a,*}, I.W.D. Dalziel ^{a,b}, P. Stone ^c, B.K. Horton ^{a,b}

- ^a Department of Geological Sciences, Jackson School of Geosciences, University of Texas at Austin, Austin, TX 78712, USA
- ^b Institute for Geophysics, Jackson School of Geosciences, University of Texas at Austin, Austin, TX 78712, USA
- ^c British Geological Survey, The Lyell Centre, Research Avenue South, Edinburgh EH14 4AP, UK

ARTICLE INFO

Article history: Received 26 September 2022 Revised 15 March 2023 Accepted 6 April 2023 Available online 8 April 2023 Handling Editor: J.G. Meert

Keywords: Falkland/Malvinas Islands Zircon Provenance Gondwana Paleogeographic reconstructions

ABSTRACT

New U-Pb geochronological, Hf isotopic, heavy mineral, and sandstone petrographic results for Paleozoic clastic deposits of the Falkland/Malvinas Islands help address renewed debates on the plate tectonic history, regional paleogeography, and basin evolution of this geologic enigma prior to Mesozoic breakup of Gondwana. The Falkland/Malvinas Islands have been considered either an autochthonous part of the South American continent or part of an independent microplate displaced from the southeastern corner of Africa. We report detrital zircon U-Pb results (n = 1306 LA-ICPMS ages) for 11 sandstone samples from the Silurian-Devonian West Falkland Group (N = 7 samples, n = 837 grains) and Carboniferous-Permian Lafonia Group (N = 4 samples, n = 469 grains). Detrital zircon age distributions for the West Falkland Group point to consistent contributions from Neoproterozoic-Cambrian (650-520 Ma) and Mesoproterozoic (1100-1000 Ma) sources. Heavy mineral assemblages and sandstone petrographic data from these samples indicate significant input from recycled sediments. A potential shift in sediment sources during deposition of the Lafonia Group is indicated by the appearance of late Paleozoic (350-250 Ma) and Proterozoic (2000–1200 Ma) age populations, decreased proportions of stable heavy minerals, and a shift to juvenile Hf values for < 300 Ma zircons. The provenance change can be attributed to the onset of subduction-related arc magmatism and potential regional shortening and crustal thickening in southwestern Gondwana during the Permian transition of a passive margin into an active, retro-arc foreland basin. The detrital zircon age distributions identified here reflect potential source regions in southern Africa and/or the Transantarctic Mountains in Antarctica. These results are most readily accommodated within a Gondwana reconstruction that includes the Falkland/Malvinas Islands as a rotated microplate originating on the eastern side of southern Africa as part of the Gondwanide foldthrust belt spanning from the Ventania region of Argentina through the Cape region of South Africa and into the Ellsworth and Pensacola mountains of Antarctica.

© 2023 International Association for Gondwana Research. Published by Elsevier B.V. All rights reserved.

1. Introduction

The Falkland/Malvinas Islands (F/MI) are an exposed part of a continental crustal block in the South Atlantic Ocean $\sim 500~km$ east of the South American mainland, situated at the base of the Falkland Plateau within the South American continental shelf (Fig. 1). The F/MI consist of two main islands, East and West Falkland, and hundreds of substantial subsidiary islands that comprise over 12,000 km^2 of land area. The geological evolution of the F/MI occurred within the context of the Gondwana supercontinent, and

E-mail addresses: joshua.malone@utexas.edu (J.R. Malone), ian@ig.utexas.edu (I.W.D. Dalziel), psto@bgs.ac.uk (P. Stone), horton@jsg.utexas.edu (B.K. Horton).

thus records similar stratigraphic patterns and structural styles preserved within South Africa, South America, and Antarctica. These intriguing structural and stratigraphic similarities raise questions about the F/MI paleogeographic position within southwestern Gondwana during the Paleozoic. There are compelling correlations among the stratigraphic and structural framework of the F/MI, Cape Fold Belt and Karoo Basin in South Africa. Adie (1952) proposed that the F/MI was situated within a rotated continental block that once lay adjacent to eastern South Africa and West Antarctica; according to this hypothesis, it was originally the eastward continuation of the Cape Fold Belt and Karoo Basin (Fig. 2). This model suggests a 180° CW rotation relative to Africa, with 120° during the Late Jurassic initial breakup of Gondwana and a subsequent 60° during opening of the South Atlantic Ocean basin.

^{*} Corresponding author.

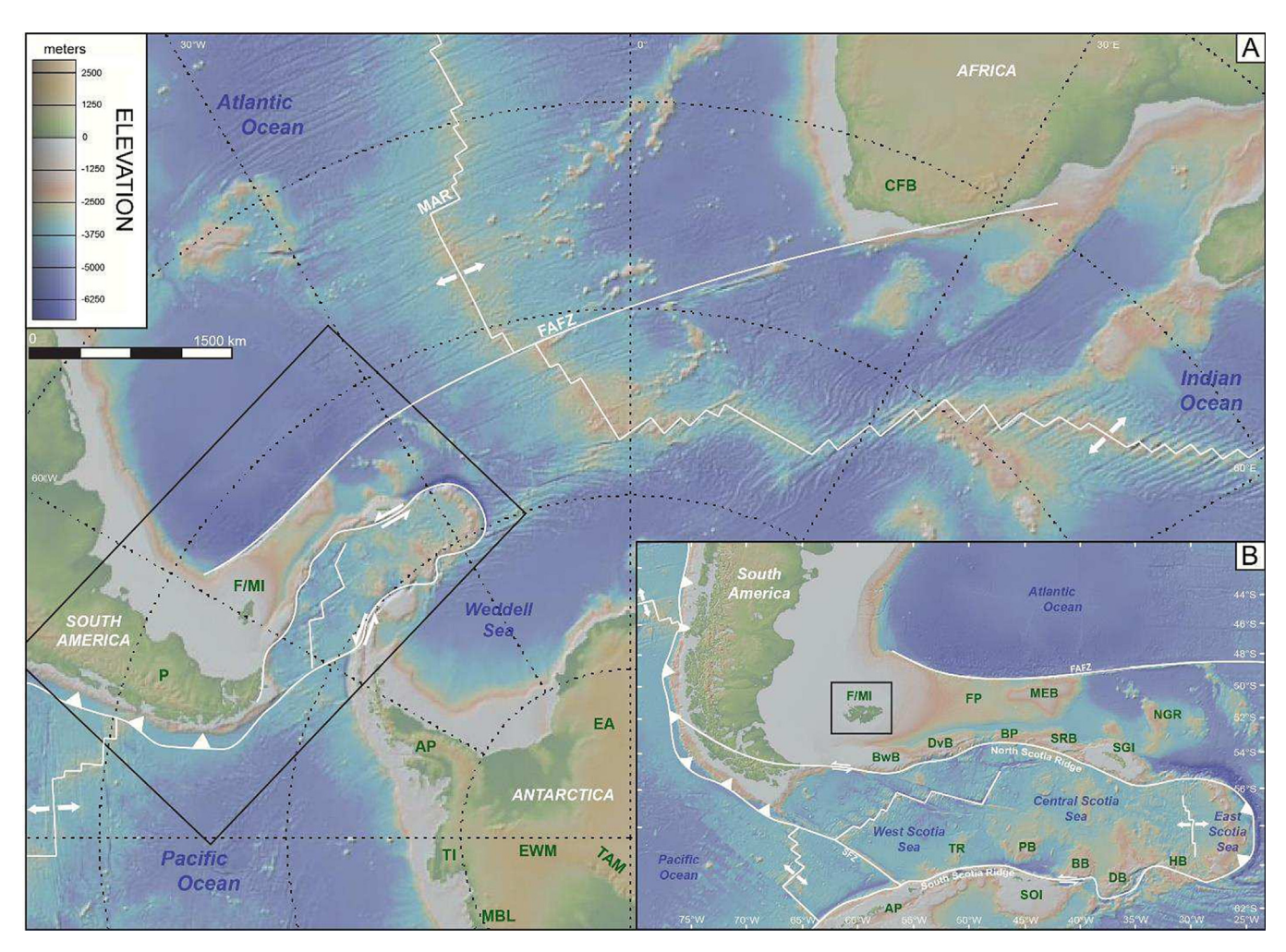


Fig. 1. A) Physiographic map of the South Pole region encompassing segments of South America, Africa, and Antarctica. B) Inset map of the Falkland/Malvinas region illustrating important physical and tectonic features: AP, Antarctic Peninsula; BP, Barker Plateau; BB, Bruce Bank; Bwb, Burdwood Bank; DvB, Davis Bank; CFB, Cape Fold Belt; DB, Discovery Bank; EA, East Antarctica; EWM, Ellsworth Whitmore Mountains; F/MI, Falkland/Malvinas Islands; FP, Falkland Plateau; HB, Herdman Bank; MBL, Marie Byrd Land; MEB, Maurice Ewing Bank; NGR, Northeast Georgia Rise; P, Patagonia; PB, Pirie Bank; SGI, South Georgia Islands; SOI, South Orkney Islands; SRB, Shag Rocks Bank; TI, Thurston Island; TR, Terror Rise; EA. Tectonic features: FAFZ, Falkland Agulhas Fracture Zone; SFZ, Shackleton Fracture Zone. Figure generated using GeoMapApp.

Many studies since have utilized a wide range of geologic techniques to support a South Africa-Antarctica placement of the F/MI (Mitchell et al., 1986; Marshall, 1994; Mussett and Taylor, 1994; Curtis and Hyam, 1998; Thistlewood and Randall, 1998; Thomson, 1998; Trewin, et al., 2002; Stone, 2016; Stanca et al. 2019, 2022). Conversely, proposed correlations with diamictites in the Sauce Grande Formation of the Ventania System and Silurian-Devonian quartzites of Sierra Grande in northern Patagonia favor a fixed position for the F/MI as a long-lived eastern promontory of southern South America (Fig. 2; Borrello, 1963; Richards et al., 1996; Lawrence et al., 1999; González et al., 2013; Ramos et al. 2017).

To help differentiate between the two contrasting models, this research aims to identify the sediment sources and tectonic setting of the F/MI prior to Mesozoic breakup of Gondwana using U-Pb detrital zircon geochronology, hafnium isotopic analysis, sandstone petrography and heavy mineral assemblages from the Paleozoic stratigraphic succession within the archipelago. An outgrowth of these efforts seeks to better resolve the Paleozoic paleogeographic position of the F/MI along the Panthalassic margin of Gondwana by comparing these results with sedimentologic, geochronological and structural data from South Africa, South America, and Antarctica.

2. Geologic setting

2.1. Regional geologic framework

The Sierra de la Ventana in Argentina, the Cape Fold Belt in southern Africa, the Ellsworth Mountains of West Antarctica, and the Pensacola Mountains along the edge of the East Antarctic craton, were all segments of an integrated late Proterozoic-Paleozoic margin that was deformed in the Permian Gondwanide orogeny (Fig. 2). The tectonic and stratigraphic evolution of the F/MI occurred within the Gondwanan supercontinent and is recorded by a \sim 15 km Paleozoic succession forming the archipelago. The Paleozoic clastic strata are cut by E-W and NE-SW Mesozoic dyke swarms (Aldiss and Edwards, 1999; Mitchell et al., 1999; Hole et al., 2016) linked to Early Jurassic breakup of Gondwana and a N-S swarm related to Early Cretaceous opening of the South Atlantic Ocean basin (Stone et al., 2009; Richards et al. 2013). The Mesozoic behavior of the F/MI remains controversial, with some arguing the F/MI were situated within a microplate that rotated 120° CW during transpression linked to initial development of the transform margin north of the islands, the Falkland-Agulhas Fracture Zone (FAFZ) (Adie, 1952; Mitchell et al., 1986; Dalziel and Grunow, 1992; Marshall, 1994; Mussett and Taylor, 1994; Thomson, 1998;

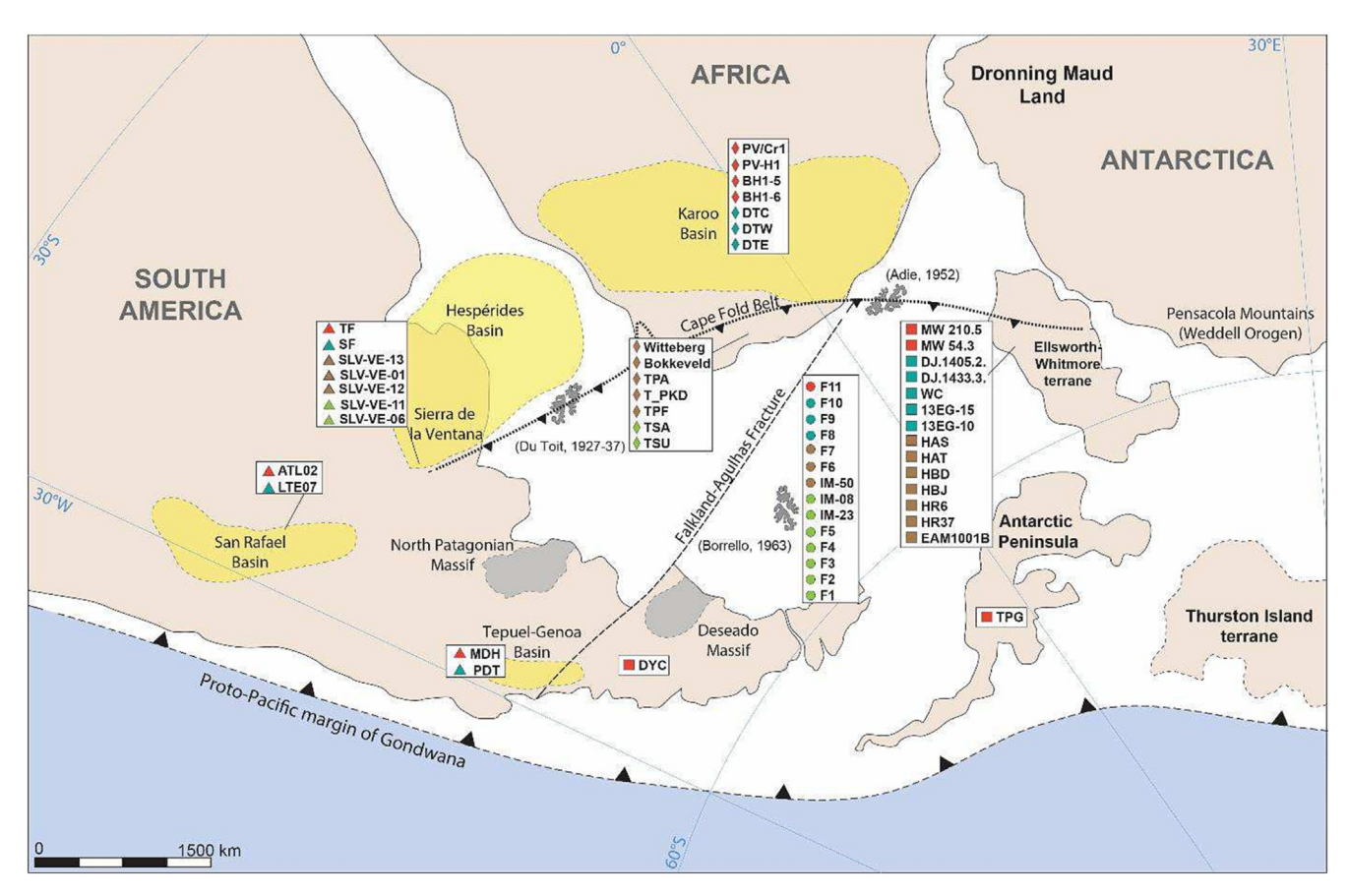


Fig. 2. Map-view paleogeographic reconstruction of the Gondwanan configuration prior to Early Jurassic breakup (modified from Dalziel et al., 2013; Stone, 2016), with three proposed original positions and orientations of the Falkland/Malvinas Islands according to Du Toit (1927, 1937), Adie (1952), and Borrello (1963) – see discussion in text. Note the position of the Antarctic Peninsula with respect to South America is poorly constrained. Also shown are sample codes for comparisons of F/MI results with the Ventania System (Ramos et al., 2014), San Rafael Basin (this study), Tepuel-Genoa Basin (Griffis et al., 2019), Patagonia (Castillo et al., 2016), Antarctic Peninsula (Castillo et al., 2016), Karoo Basin (Nxumalo, 2012; Viglietti et al., 2018; Craddock et al., 2019), Cape Fold Belt (Fourie et al., 2011; Vorster et al., 2021) and the Ellsworth Mountains (Elliot et al., 2016; Craddock et al., 2017; Castillo et al., 2017).

Curtis and Hyam, 1998; Storey et al., 1999; Trewin et al., 2002; Macdonald et al., 2003; Stone et al., 2009; Stanca et al., 2019, 2022). The dearth of evidence for a major structural break, notably one demonstrating compression, between the F/MI and South American continent led others to support a more conservative, non-rotational model that places the F/MI in a fixed location relative to South America as it is today (Lawrence et al., 1999; Ramos et al., 2017; Lovecchio et al., 2019; Eagles and Eisermann, 2020). Nonetheless, the Paleozoic stratigraphic evolution of the F/MI precedes supercontinent fragmentation and is recorded within Silurian-Permian clastic strata potentially derived from various crustal provinces of South America, Africa, and Antarctica, Key provinces mentioned in this study include: the Falkland/Malvinas Islands (F/MI), Ellsworth Whitmore terrane (EWT), Antarctic Peninsula (AP), Dronning Maud Land (DML), Cape Fold Belt (CFB), Karoo Basin, and Sierra de la Ventana (Ventania) System (Fig. 2).

2.2. Falkland-Malvinas Islands stratigraphic framework

The geologic configuration of the Falkland/Malvinas Islands (F/MI; Fig. 3) was surveyed and described in detail by Aldiss and Edwards (1999) and reviewed by Stone (2016). The onshore geology of the F/MI consists of a Mesoproterozoic basement, c. 1000 Ma (Cingolani and Varela 1976; Jacobs et al. 1999), which is overlain by the \sim 7500 m thick Silurian–Devonian West Falkland Group. The West Falkland Group consists of fluvial to shallow marine quartzites, sandstones and mudstones deposited within a

broad passive margin encompassing South America, South Africa, and Antarctica. A low angle unconformity separates the West Falkland Group from the overlying ~ 7500 m thick Carboniferous-Permian Lafonia Group, which has glaciogenic units at its base, proglacial sediment and diamictite, and then passes upsection into deltaic and lacustrine sandstones and mudstones deposited in a foreland basin setting. While the mechanism generating the F/MI low-angle unconformity is unknown, unconformity-bounded megasequences in the Cape and Karoo basins indicate a threestage evolution over a 200 Myr timescale, including crustal uplift (~3km), fault-controlled subsidence, and long periods of regional subsidence with minor faulting (Tankard et al., 2009), Improved assessments of the proximity of the F/MI to the Cape and Karoo basins throughout the Paleozoic are required to determine whether the F/MI shared a similar tectonic history as southern Africa.

2.2.1. West Falkland Group

The Silurian to Devonian West Falkland Group consists of four lithostratigraphic units: (1) Port Stephens, (2) Fox Bay, (3) Port Philomel, and (4) Port Stanley formations. The lower levels of the West Falkland Group, defined by the \sim 4500 m thick Port Stephens Formation, are exposed in West Falkland (Isla Gran Malvina) (Fig. 3) and the northern half of East Falkland (Isla Soledad). The principal lithologies include quartzitic to quartzofeldspathic sandstones, granule to pebble conglomerates, and mudstones (Aldiss and Edwards, 1999; Hunter and Lomas, 2003; Stone, 2016).

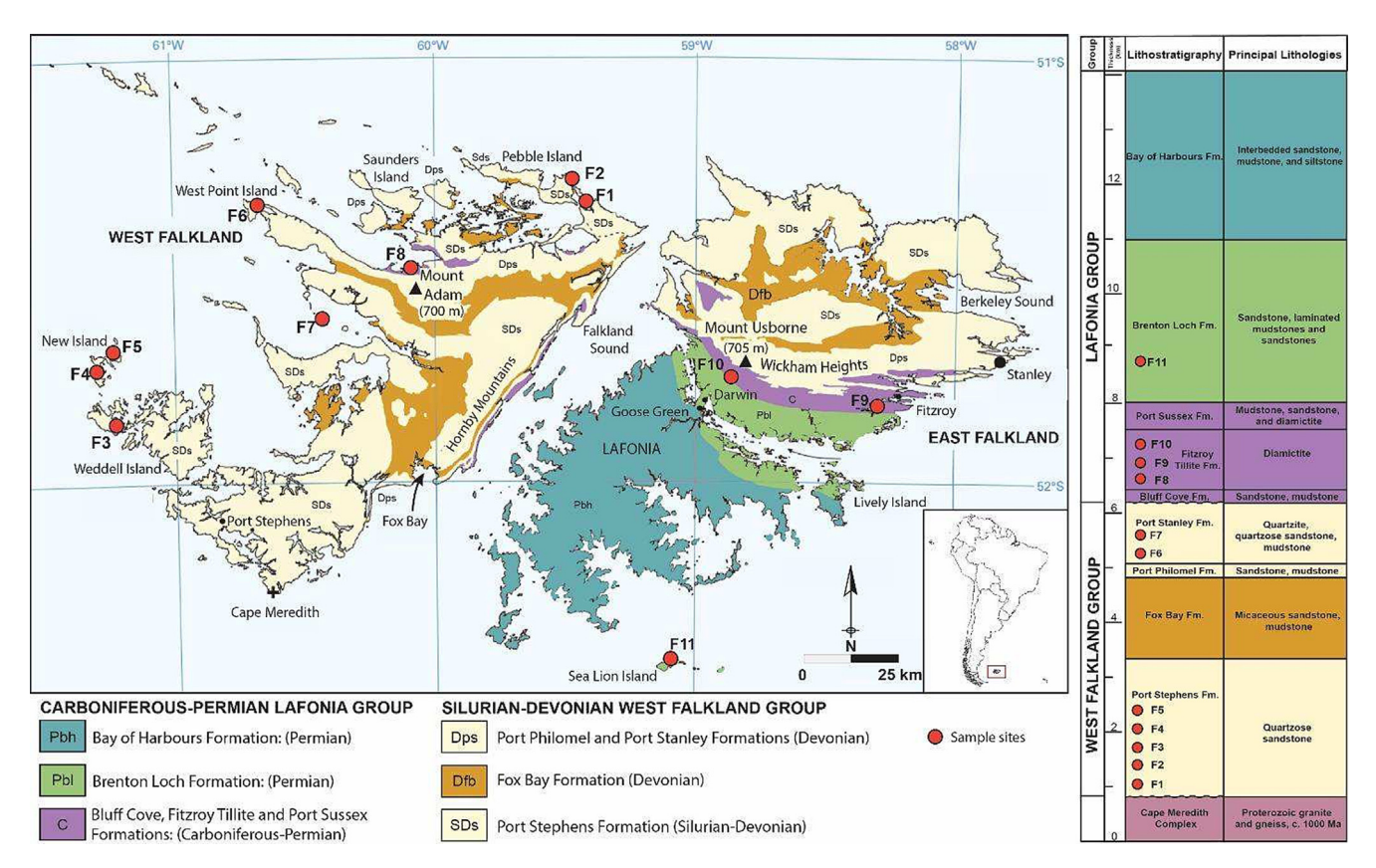


Fig. 3. Geologic map of the Falkland-Malvinas Islands with sample locations marked by circles (modified from Aldiss and Edwards, 1999 and Stone, 2016).

Geochronological studies from Silurian dykes cutting the Cape Meredith Complex indicate a 422 ± 39 Ma maximum age for the basal Port Stephens Formation (Stone, 2016). Depositional environments included fluvial and shallow marine conditions when the region was a broad alluvial to coastal plain, deepening to the present-day NE (Hunter and Lomas, 2003). Differences in heavy mineral content indicate some provenance variations, but the dominance of mature sandstones suggests a stable cratonic source (Aldiss and Edwards, 1999).

The Port Stephens Formation is conformably overlain by the Fox Bay and Port Philomel formations, which crop out throughout West Falkland and the northern half of East Falkland (Fig. 3). The Fox Bay and Port Philomel depositional environment was mainly a shallow marine system, ranging from inner shelf to shoreface (Aldiss and Edwards, 1999). A widespread Early Devonian (Pragian-Emsian) fossil fauna in the Fox Bay Formation was discovered by Charles Darwin in 1833 during the voyage of HMS *Beagle* (Darwin, 1846; Morris and Sharpe, 1846). The Port Philomel Formation is locally rich in plant material.

The Port Stanley Formation defines the upper WFG and is equally exposed throughout the northern half of both East and West Falkland. Principal lithologies include pale grey quartzites and quartz rich sandstones, interbedded with siltstones and mudstones (Aldiss and Edwards, 1999; Stone, 2016). Depositional environments ranged from marine shoreface with tidal channels (Aldiss and Edwards, 1999) to braided fluvial channel systems (Meadows, 1999). Biostratigraphic palynological data from intermediate to upper levels of the West Falkland Group indicate minimum depositional ages of Givetian (Middle Devonian) for the top of the Port Philomel Formation and Famennian (Late Devonian) near the top of the Port Stanley Formation (Marshall, 2016).

2.2.2. Lafonia Group

The Carboniferous to Permian Lafonia Group comprises five principal lithostratigraphic units: (1) Bluff Cove, (2) Fitzroy Tillite, (3) Port Sussex, (4) Brenton Loch and (5) Bay of Harbours formations. The lower Lafonia Group, defined by the Bluff Cove, Fitzroy Tillite and Port Sussex formations, consists mainly of quartzofeldspathic sandstone, laminated siltstone, mudstone, and sandy diamictite containing a variety of matrix-supported erratic clasts (Frakes and Crowell, 1967; Aldiss and Edwards, 1999; Meadows, 1999: Stone, 2016). The basal unit, the Bluff Cove Formation. exposed only in East Falkland (Fig. 3), is interpreted as a proglacial deposit (glaciomarine or glaciolacustrine) due to the increasing proportions of dropstones upsection into the Fitzroy Tillite (Aldiss and Edwards, 1999). Dropstone lithologies in the Fitzroy Tillite vary among sandstone, quartzite, and various granitic rocks. Metamorphic clasts are also present, more commonly in diamictite outcrops of West Falkland than in East Falkland. There are also diagnostic fossiliferous limestone clasts containing an early Cambrian archaeocyath-trilobite fauna (Stone and Thomson, 2005; Stone et al., 2012). The archaeocyath limestone clasts were thought to originate in the Transantarctic Mountains as 12 of 19 forms in the diamictite of the F/MI have close correlatives in the Transantarctic Mountains and erratics derived therefrom (Stone and Thomson, 2005; Stone et al., 2012). Rodríguez-Martínez et al. (2022) have recently reported that of 16 genera described from the Falkland Island diamictites, 3 are shared with those from the newly discovered former siliciclastic-carbonate platform in the Shackleton Range. Transantarctic archaeocyathans have also been reported from Permo-Carboniferous diamictites in Argentina, Namibia and South Africa (González et al., 2013; Cooper and Oosthuizen, 1974; Perejón et al., 2019). Others found in

Cambro-Ordovician metaconglomerates in northern Patagonia are also believed to be allochthonous (González et al., 2013).

The Brenton Loch and Bay of Harbours formations constitute the upper Lafonia Group. The Brenton Loch Formation contains volcanic-rich feldspathic lithic arenites, siltstones, and mudstones, all deposited within a pro-deltaic system as delta-derived turbidites or interbedded rhythmite accumulations (Aldiss and Edwards, 1999; Trewin et al., 2002). A varied ichnofauna and rare bivalve fossils (Simões et al. 2012) support a lacustrine environment in an overall pro-deltaic succession (Trewin et al., 2002). The Bay of Harbours Formation represents a prograding delta front transitioning into a meandering delta-top channel system (Aldiss and Edwards, 1999; Trewin et al., 2002). The dominant siltstone, mudstone, and volcaniclastic-rich sandstone lithologies are like those of the Brenton Loch Formation.

2.3. Potential sediment sources

The development of the southwestern Gondwanan margin provides a framework for understanding potential sources of sediment to the F/MI prior to breakup of Gondwana (Fig. 2). The Ediacaran to Cambrian amalgamation of internal Pan-African orogens provided the structural foundation of the Gondwana supercontinent (Kröner and Stern, 2004; Cawood and Buchan, 2007; Goscombe et al., 2020; Sundell and Macdonald, 2022). The Pan-African orogens developed during Neoproterozoic rifting of Rodinia (850-600 Ma; Condie, 2005; Li et al., 2008) and exist primarily in southern Africa (Gariep, Damara, Saldania and Mozambique belts) and eastern South America (Dom Feliciano and Brasilia belts). The external Cambrian-Ordovician Ross-Delamerian orogen in Antarctica and Australia outlines the rifted Rodinian margin. These orogens supplied sediment to Neoproterozoic-Cambrian successions in Namibia and South Africa (Nama, Port Nolloth, Oranjemund, Boland groups) along continental margins and within intracratonic basins that underwent several stages of erosional recycling throughout the Phanerozoic and Cenozoic (Andersen et al., 2016a, 2016b, 2018a, 2018b; Kristoffersen et al., 2016).

The timing and duration of magmatism and terrane accretion provide additional insights into evolving sediment sources as the region transitioned from a passive margin to a foreland basin. The two major Paleozoic tectonic phases along the Paleo-Pacific Margin include: (1) Cambrian-Devonian terrane accretion and (2) Carboniferous-Permian subduction (Schwartz et al., 2008; Ducea et al., 2010; Alasino et al., 2012; Dahlquist et al., 2013; del Rey et al., 2016; Rapela et al., 2016; Capaldi et al., 2021). Pampean (555–515 Ma) and Famatinian (460–440 Ma) orogenesis preceded and accompanied Ordovician accretion of the Cuyania terrane to the pre-Andean margin (Thomas et al., 2015; Rapela et al., 2016; Martin et al., 2019). The timing of renewed subduction during the Carboniferous ranges between 343 and 310 Ma (Willner et al., 2008, 2012) and is associated with slab rollback and upper-plate extension along the Gondwanan plate margin (Dahlquist et al., 2013; del Rey et al., 2016). This is recorded through Carboniferous-Permian granitoids and orthogneisses in eastern Marie Byrd Land, Thurston Island, Antarctic Peninsula, and southern South America (Riley et al., 2012; Chernicoff et al., 2013; Elliot, 2013; Elliot et al., 2016). The cessation of Carboniferous magmatism was associated with a period of flat-slab subduction, leading to the Gondwanide Orogeny (~285-270 Ma; Dalziel et al., 2000) and development of the Gondwanide fold-thrust belt. The last major episode of Paleozoic magmatism is exemplified by the Choiyoi igneous complex (270-240 Ma), an extensive ignimbrite flareup likely driven by crustal thinning and upper-plate extension during subducting slab rollback and lithosphere delamination beneath Gondwana (Kleiman and Japas, 2009; del Rey et al., 2016; Nelson and Cottle, 2019; Capaldi et al., 2021). Given

the spatial distribution of accreted terranes and orogens throughout SW Gondwana, we consider the Pan-African orogens, Neoproterozoic-Cambrian siliciclastic successions within southern Africa, Paleozoic accreted terranes (Pampia, Famatinia, and Cuyania) and the late Carboniferous-early Permian magmatic arc as potential sediment sources to the F/MI during its Paleozoic evolution from a passive margin to a foreland basin.

2.4. Competing paleogeographic positions

2.4.1. Adie (1952)

The paleogeographic reconstruction of Du Toit (1927, 1937) first positioned the Falklands significantly north of their present location, situated between the Sierra de la Ventana fold belt of Argentina and the Cape Fold Belt of South Africa (Fig. 2). This reconstruction is untenable in terms of a modern understanding of the opening of the Atlantic Ocean basin, but even before the advent of plate tectonics it had been much criticized and widely dismissed by Du Toit's contemporaries. Adie (1952) supplied an alternative reconstruction in which the Falkland Islands are the direct eastward continuation of the Cape Fold Belt and Karoo Basin, and after comparison of sedimentological and structural data, rotated the archipelago 180° CW into a geologically preferred position (Fig. 2). The Adie (1952) reconstruction solved one of the issues that had undermined the Du Toit (1927, 1937) model: whereas the Cape Fold Belt verges northward toward the Karoo foreland basin (with a similar regional arrangement as the Sierra de la Ventana), in the current Falkland/Malvinas Islands, the fold belt verges southward toward foreland basin fill of the Lafonia Group. Adie had described a rotated microplate, but it would be another decade before the realization of plate tectonics accommodated such a phenomenon, and the exact mechanism for microplate rotation is still not readily apparent.

2.4.2. Borello (1963)

Instead of a South African link for the F/MI geology, opinion strengthened that the archipelago lay on a fixed promontory extending from the Deseado Massif of Argentina, a view exemplified by Borrello (1963) and one to which Adie apparently came to acquiesce (Stone, 2021). Then came the first palaeomagnetic data from Jurassic dykes in the Falkland Islands, which were taken to confirm rotation, and Adie's (1952) reconstruction was revivified (Mitchell et al., 1986; Taylor and Shaw, 1989). Thereafter, and particularly following the geological resurvey by Aldiss and Edwards (1999), a wide range of geological studies produced compelling correlations with South Africa in terms of lithostratigraphy (Trewin et al., 2002; Hunter and Lomas, 2003), structure (Curtis and Hyam, 1998) and the magnetic characteristics of the dyke swarms (Stone et al., 2009). Nevertheless, dissent continued, and was initially strengthened by the expanding database arising from offshore hydrocarbon exploration. Early results seemed to preclude microplate rotation as no evidence of this was found in offshore geophysical studies (Richards et al., 1996), but some of the latest interpretations have proved not only more favorable to Adie's reconstruction, albeit with some modification, but also identified structures that could accommodate the rotational deformation (Stanca et al., 2019, 2022). Conversely, the case for the South American correlation of the Falkland Islands has been maintained and developed, amongst others by Ramos et al. (2017, 2019); this model requires the coeval but independent development of a south-verging fold-thrust belt and foreland basin with the same stratigraphy and structure as the north-verging Cape-Karoo system.

3. Methods

Eleven sandstone samples from the F/MI are subdivided into eight samples of Silurian-Permian strata collected by Ian Dalziel (University of Texas at Austin) in 2019 on a private yacht cruise around the F/MI, and three from the Fitzroy Tillite provided by Philip Stone (British Geological Survey) from material collected during a mineral exploration program (Fig. 3; Table 1). The eleven samples include seven from the West Falkland Group and four from the Lafonia Group. Given the regional uniformity of Gondwanan sediment sources in terms of U-Pb age distributions, a more robust provenance analysis is aided by Lu-Hf-Yb isotopic analyses, heavy mineral assemblages, and sandstone petrography. All eleven samples were analyzed for detrital zircon U-Pb geochronology, with four selected for Lu-Hf-Yb isotopic analyses (F2, F6, F8, F11) and nine selected for heavy mineral and sandstone petrographic

analyses (F1-F8, F11). U-Pb ages from an additional forty-four samples from published literature (Fig. 4; see Appendix A), including three from the F/MI from Ramos et al. (2017), provide the basis for a statistical comparison with the new results from this study.

3.1. U-Pb geochronology

U-Pb geochronological analyses were conducted on detrital zircon grains from all eleven samples. Following traditional physical and chemical mineral density separation techniques (including water table, heavy liquid and magnetic separation), a selection of inclusion-free zircon grains of variable size and shape were randomly selected and analyzed for U-Pb geochronology on the Element 2 LA-ICPMS (inductively coupled plasma mass spectrometer), with subsequent Lu-Hf-Yb isotopic analyses on the Nu Plasma HR multicollector ICPMS at the University of Arizona

Table 1Sample codes, coordinates, and lithologies for Silurian to Permian stratigraphic units sampled within the Falkland/Malvinas Islands. Original sample ID's were assigned 'new' sample ID's to indicate stratigraphic position relative to each other (F1 = oldest, F11 = youngest).

ORIG_ID	NEW_ID	Age	Unit	Lat (DD)	Long (DD)	Lithology
F8	F11	Carboniferous-Permian	Brenton Loch Formation, Lafonia Gp.	-52.446617	-59.1145	sandstone
F10	F10	Carboniferous (BGS)	Fitzroy Tillite, Lafonia Gp.	-51.743056	-58.876389	diamictite matrix
F9	F9	Carboniferous (BGS)	Fitzroy Tillite, Lafonia Gp.	-51.811111	-58.327778	diamictite matrix
F11	F8	Carboniferous (BGS)	Fitzroy Tillite, Lafonia Gp.	-51.502778	-60.124444	sandstone
F6	F7	Devonian	Port Stanley Fm. West Falklands Gp.	-51.618283	-60.433683	sandstone
F3	F6	Devonian	Port Stanley Fm. West Falklands Gp.	-51.354667	-60.680983	quartzite
F5	F5	Silurian	South Harbour Mbr, Port Stephens Fm., West Falklands Gp.	-51.688733	-61.254217	conglomerate
F4	F4	Silurian	South Harbour Mbr, Port Stephens Fm., West Falklands Gp.	-51.721867	-61.3009	sandstone
F7	F3	Silurian	Port Stephens Fm., West Falklands Gp.	-51.8529	-61.24735	quartzite
F2	F2	Silurian	Port Stephens Fm., West Falklands Gp.	-51.284233	-59.477833	quartzite
F1	F1	Silurian	Port Stephens Fm., West Falklands Gp.	-51.321233	-59.443583	quartzite

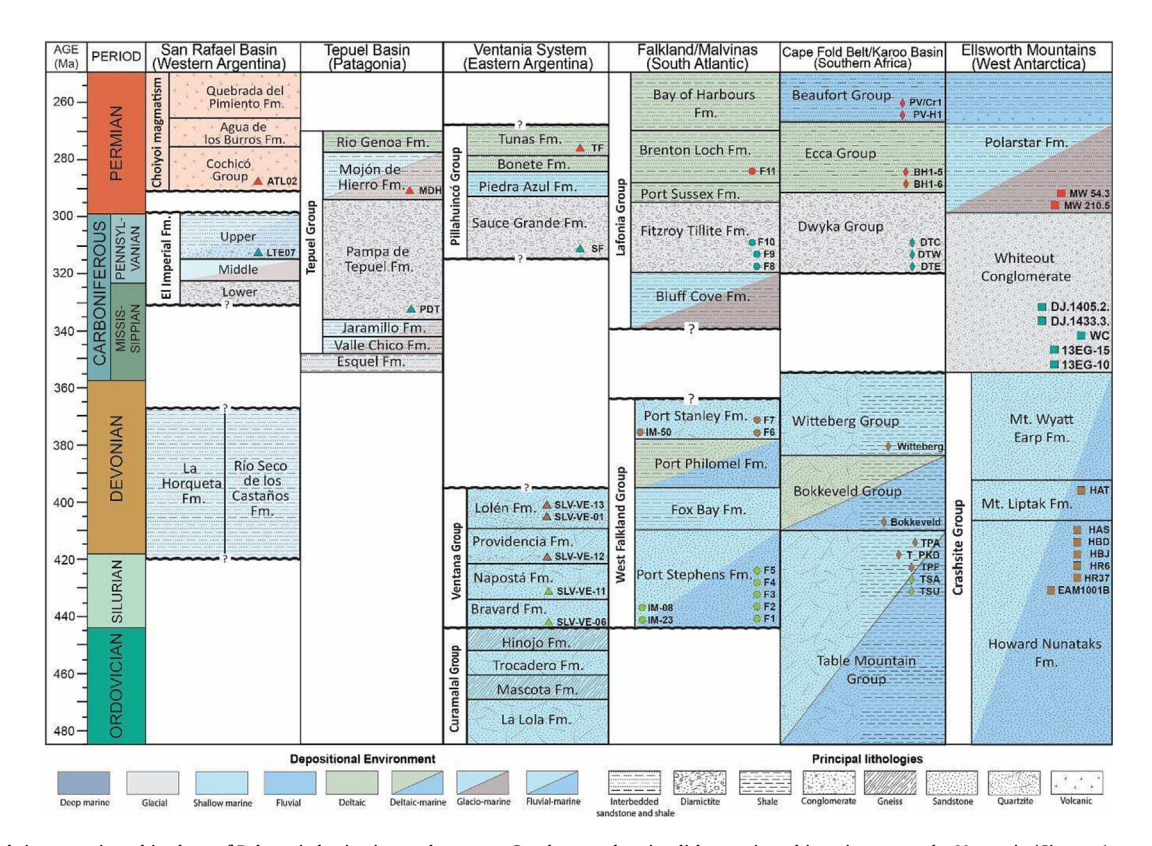


Fig. 4. Regional time-stratigraphic chart of Paleozoic basins in southwestern Gondwana, showing lithostratigraphic units across the Ventania (Sierras Australes, Argentina), San Rafael Basin (Western Argentina), Tepuel-Genoa Basin (Patagonia), Cape Fold Belt (South Africa), Karoo Basin (South Africa), Ellsworth Mountains (West Antarctica) and the Falkland/Malvinas Islands. After Ramos et al. (2014), Stone (2016), Tankard et al. (2009), Curtis and Lomas (1999), Craddock et al. (2017), Elliot et al. (2013).

LaserChronCenter (Gehrels et al., 2006, 2008; Gehrels and Pecha 2014, and Cecil et al., 2011). We report 1306 new U-Pb geochronological results with measured age uncertainties of 1-2% (1σ error). We use 206Pb/238U ages for zircons younger than 900 Ma and 206Pb/207Pb ages for zircons older than 900 Ma. Individual analyses were filtered such that results displaying > 20% discordance, >5% reverse discordance were excluded from further consideration. Data reduction was conducted using AgeCalcML software (Sundell et al., 2021).

3.2. Hafnium isotopic analysis

Hf isotopic results are reported in epsilon units (ϵ) and presented in Hf evolution diagrams as ϵ Hf(t) values representing the isotopic composition at the time of crystallization (t) in reference to CHUR (chondritic uniform reservoir; Bouvier et al., 2008), DM (depleted mantle; Vervoort and Blichert-Toft, 1999), and average crustal evolution (assuming modern 176Lu/177Hf = 0.0115; Vervoort and Patchett, 1996; Vervoort and Blichert-Toft, 1999). Measured 176Hf/177Hf uncertainties are \sim 1 epsilon unit (1 ϵ).

3.3. Sandstone petrography

Nine samples were selected for sandstone petrography. Each sample was point-counted for 350 grains using the Gazzi-Dickinson method (Ingersoll et al., 1984; Garzanti, 2019) using conventional grain classifications (see Appendix E). Each sample was stained for calcium and potassium feldspar. Lithologies of the point counted samples were quartzite (five), sandstone (three) and conglomerate (one). Two samples (F10 and F11) were unable to be point counted due to limited grain sizes needed for accurate characterization. Point-count results are represented on QFL, QmFLt and LmLsLv ternary diagrams (constructed in Microsoft Excel [Version 2112]) to interpret and characterize sediment sources initially outlined in Dickinson and Suczek (1979); Dickinson et al., (1983).

3.4. Heavy mineral analysis

Heavy mineral assemblages were assessed for nine samples. Each sample was crushed, pulverized, and subjected to physical and chemical mineral density separation techniques (water table differentiation, then further separation using liquid bromoform). Heavy mineral separates (density $\geq 2.89~\text{g/cm}^3$) (Morton and Hallsworth 1994; 1999) were sent to the Automated Mineralogy Facility (AMF) at the Colorado School of Mines for analysis. Each sample was processed using TIMA and QEMSCAN techniques (Allen et al., 2012; Bush et al., 2016) to extrapolate the mass, volume, and total grain percentages. Raw data generated by the AMF was reduced by removing non-heavy (<2.9~g/cm3) and diagenetic minerals.

3.5. Statistical analysis of U-Pb age spectra

Three statistical techniques were employed to evaluate the similarities among detrital zircon age distributions obtained from this and previous studies: multi-dimensional scaling (MDS), Kolmogorov-Smirnov (K-S) statistics, and the overlap of confidence intervals of empirical cumulative distributions (O). Given a table of pairwise 'dissimilarities', the MDS technique utilizes principal component analysis (PCA) and produces a dimensionless map of points on which samples with statistically similar age distributions cluster close together and statistically dissimilar samples plot farther apart (Vermeesch, 2012). MDS plots were constructed with DZmds (Saylor et al., 2018) using probability density plot cross-correlation and the optimum number of dimensions to reduce

stress. The K-S test utilized in this study follows the approach outlined by Guynn and Gehrels (2010), which compares two sample age distributions to determine if there is a statistically significant difference between the two samples. The fundamental measure for the K-S test is the P value: if the P-value is < 0.05, the level of confidence that the two age distributions are not the same (do not share similar provenance) is > 95%. The degree of overlap (O) measures the combined lengths of intervals along the cumulative age distributions within which the 95% confidence intervals overlap (Andersen et al., 2018a). This test generates a '1-O' value, which reports the measure of relative overlap of confidence intervals between two samples. Sample comparisons where 'O = 1', or '1 - O = O', indicate complete overlap.

The MDS approach in this study utilizes probability density plot cross-correlation, which can be sensitive to a sample size below n = 300 (Saylor and Sundell, 2016), but provides the most dependable method for assessing similarity among multiple samples (Saylor and Sundell, 2016). Comparisons using the K-S test are a preferred method for comparison between two samples (Vermeesch et al., 2016), but are also sensitive to sample size. The '1-0' test compares overlap between the 95% confidence bands of cumulative density functions, in which the half-width of the confidence band is a function of the number of analyses in each sample (Andersen et al., 2016a). Together, these three statistical approaches are applied to discrete intervals of geologic time, (1) Silurian, (2) Devonian, (3) Carboniferous and (4) Permian, to maximize the practical functionality of each approach.

4. Results

We report here U-Pb geochronologic, Hf-Lu isotopic, heavy mineral, and sandstone petrographic results from a suite of samples spanning the Paleozoic stratigraphic succession of the F/MI. Ramos et al. (2017) provided the first U-Pb and Hf-Lu detrital zircon geochronological results for the West Falkland Group, however, our study aims to build upon these data and re-evaluate hypotheses concerning the F/MI paleo-position prior to breakup of Gondwana.

4.1. U-Pb geochronology

4.1.1. West Falkland Group

Seven WFG samples include five from the Silurian Port Stephens Formation (F1, F2, F3, F4, F5; n = 599 analyses) and two from the Devonian Port Stanley Formation (F6 and F7, n = 237 analyses). Detrital zircon U-Pb results for all seven WFG samples exhibit consistent bimodal age distributions (Fig. 5a), with Neoproterozoic-Cambrian (750–500 Ma) and late Mesoproterozoic spectral age peaks (1150–1050 Ma). Smaller Neoproterozoic (920, 915, 823, and 817 Ma) age peaks are present as well. Composite age probability plots for Silurian and Devonian samples (Fig. 5b) help delineate four principal age peaks at \sim 561, \sim 650, \sim 730, and 1072 Ma.

4.1.2. Lafonia Group

Four samples from the Lafonia Group include three from the Carboniferous Fitzroy Tillite (F8, F9 and F10; n = 340 analyses) and one from the Permian Brenton Loch Formation (F11; n = 129 analyses). Principal U-Pb age peaks within the Fitzroy Tillite include $\sim 535, \sim 634,$ and 1091 Ma peaks. Increased proportions of Archean ages (n = 6 grains; 3317–2506 Ma) and Paleoproterozoic zircon grains (n = 29; 2461–1600 Ma) exist within the Fitzroy Tillite. Zircon grains from the Brenton Loch Formation exhibit three dominant age peaks at $\sim 269, \sim 337,$ and ~ 534 Ma, with subordinate age peaks at $\sim 762, \sim 850,$ and ~ 1000 Ma.

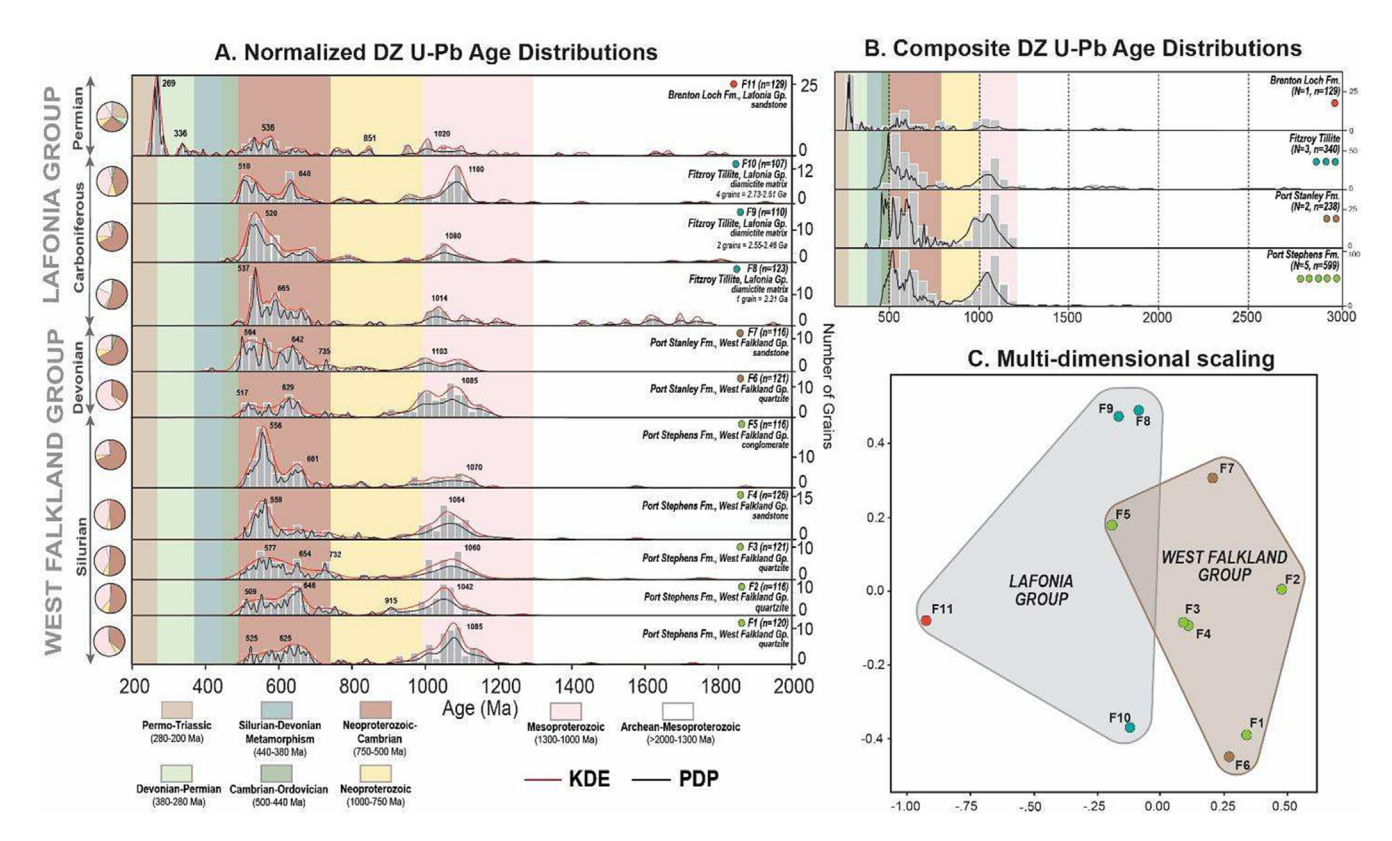


Fig. 5. A.) Detrital zircon U-Pb age distributions depicted as normalized age probability (black line) and kernal density (red line) functions and age histograms (shaded gray rectangles). Pie charts display relative zircon age proportions for each sample. B.) Non-normalized PDP's and histograms displaying the most prominent age modes (<250 Ma) for samples collected in the Silurian, Devonian, Carboniferous, and Permian. C.) Multidimensional scaling (MDS) plot of all samples shown in (A). Basis for comparison is cross-correlation of probability density plots. Plots in both (A) and (B) generated using python-based program detritalPy (Sharman et al., 2018). MDS Plot constructed using DZmds (Saylor and Sundell, 2016). (For interpretation of the references to color in this figure legend, the reader is referred to the web version of this article.)

4.2. Hafnium isotopic analysis

Four samples (F2, F6, F8 and F11) were selected for Hf isotopic analyses to assess Paleozoic crustal evolution and magmatic patterns recorded by the F/MI clastic succession. A total of 212 analyses from the F/MI (Fig. 6a) are combined with 1,225 published isotopic results from detrital samples in the Table Mountain Group (South Africa; Vorster et al., 2021), Nama Group (Namibia; Andersen et al., 2018b), Crashsite Group (West Antarctica; Flowerdew et al., 2007), Trinity Peninsula Group (West Antarctica; Bradshaw et al., 2012; Castillo et al., 2016), Duque de York Complex (Castillo et al., 2016) and Ventana Group (Ventania System; Uriz et al., 2011; Ramos et al., 2014) into a single Hf evolution diagram. Considering a composite U-Pb age distribution allows for the discrimination of three dominant age groups and corresponding Hf values within the F/MI: (1) 274–253 Ma, ε Hf(t) = -2.34–10.2 range (3.3 mean); (2) 650–500 Ma, ε Hf(t) = -31.4–15.1 range (0.18 mean), and (3) 980-1105 Ma, $\varepsilon Hf(t) = -30.34-14.6$ range (4.4 mean).

These results can be compared with transitions in magmatic behavior in SW Gondwana, based on a compilation of published hafnium isotopic ages (Fig. 6b). We highlight several key observations regarding the crustal evolution recorded by the F/MI sediments:

- (1) Between \sim 1.75 and 1.2 Ga, ϵHf values become progressively more positive, reflecting gradual incorporation of more juvenile magmas.
- (2) From 1250 to 500 Ma, a clear trend from moderately positive to slightly negative εHf values (-5.4–15.9 range) indicates an average crustal evolution trajectory (Fig. 6), consistent with

reworking of older crustal sources rather than generation of new crustal sources.

(3) A rapid increase (isotopic pullup) in juvenile magmatism (-2.3–10.2 ϵ Hf range) is defined by a major phase of late Paleozoic (\sim 286–253 Ma) magmatism.

The analyzed F/MI zircons show temporal trends most like ϵ Hf signatures from the Crashsite and Trinity Peninsula groups, the latter being a Carboniferous-Triassic metasedimentary succession in the northern Antarctic Peninsula of importance for reconstructions of the Pacific margin of Gondwana (Castillo et al., 2015).

4.3. Sandstone petrography and heavy mineral analysis

Sandstone compositional data and heavy mineral proportions supplement U-Pb ages and hafnium isotopic ages to further characterize potential sediment sources and temporal trends. Sandstone compositions throughout the West Falkland and Lafonia Groups are strikingly similar with minimal differences in grain variety (Fig. 7a). Dominant grains consist mostly of monocrystalline quartz and sedimentary lithic fragments (mostly claystone and siltstone fragments). Upsection trends in Carboniferous samples F9 and F10 show increased proportions of plagioclase (14% and 4.8%, respectively) and potassium feldspar (4% and 10%, respectively) relative to the WFG. Similarly, sandstone compositions also show an increase in metamorphic lithic proportions from Silurian to Carboniferous units.

Heavy mineral assemblages for seven samples in the WFG (F1-F7) and two samples in the Lafonia Group (F8 and F11) yield a diverse suite of: (1) unstable minerals (biotite, chlorite, amphibole, pyroxene, enstatite), (2) stable minerals (apatite, garnet, titanite,

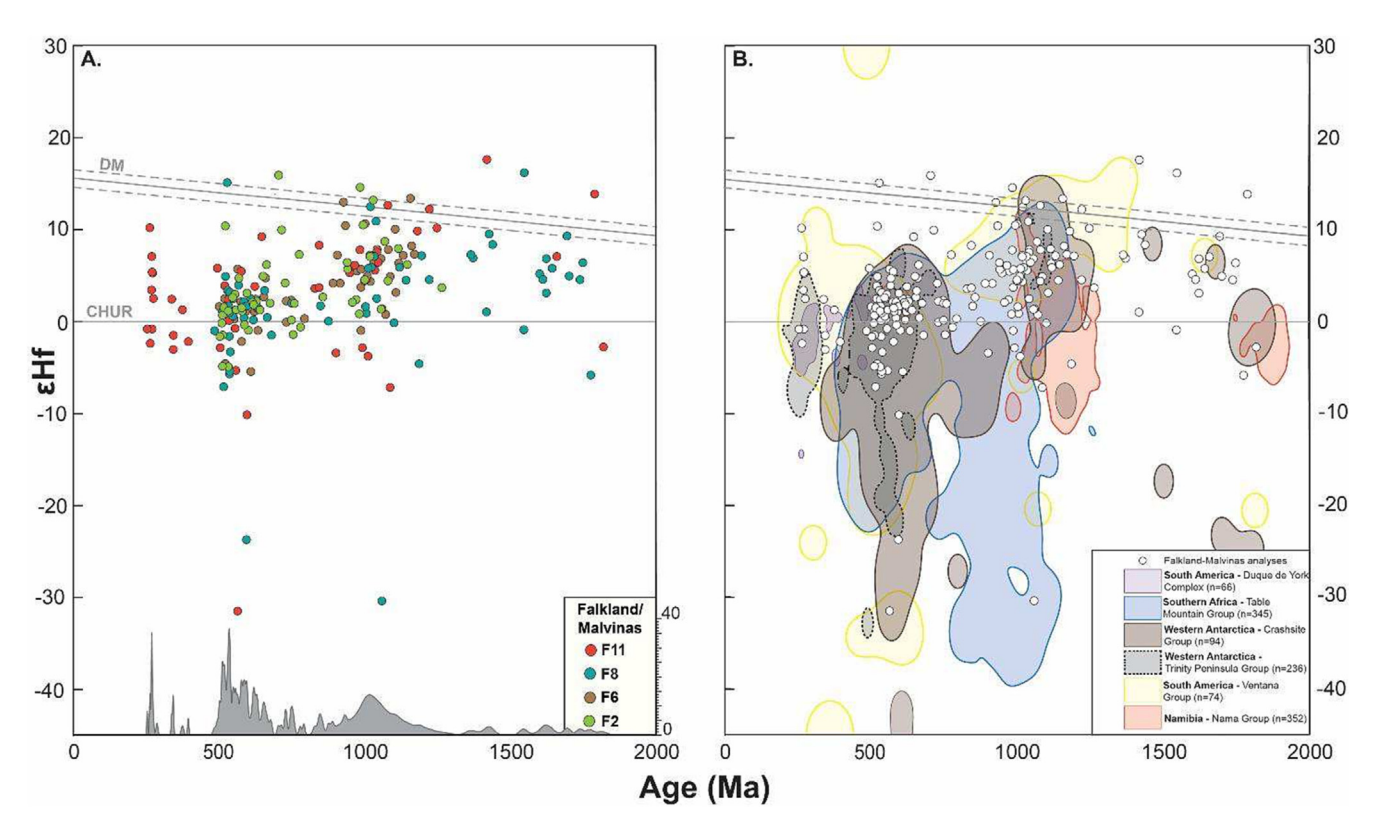


Fig. 6. A.) εHf(t) vs. U-Pb crystallization ages of detrital zircons from the Port Stephens formation (F2), Port Stanley formation (F3), Fitzroy Tillite (F8) and Brenton Loch formations (F11). B.) Comparative εHf(t) evolution diagrams showing all Falkland-Malvinas values relative to 95% contour levels of εHf(t) values from detrital zircons within time-correlative units in the Table Mountain Group (South Africa; Vorster et al., 2021), Nama Group (Namibia; Andersen et al., 2018b), Crashsite Group (West Antarctica; Flowerdew et al., 2007), Trinity Peninsula Group (West Antarctica; Bradshaw et al., 2012; Castillo et al., 2016), Duque de York Complex (Castillo et al., 2016) and Ventana Group (Ventania System; Uriz et al., 2011; Ramos et al., 2014).

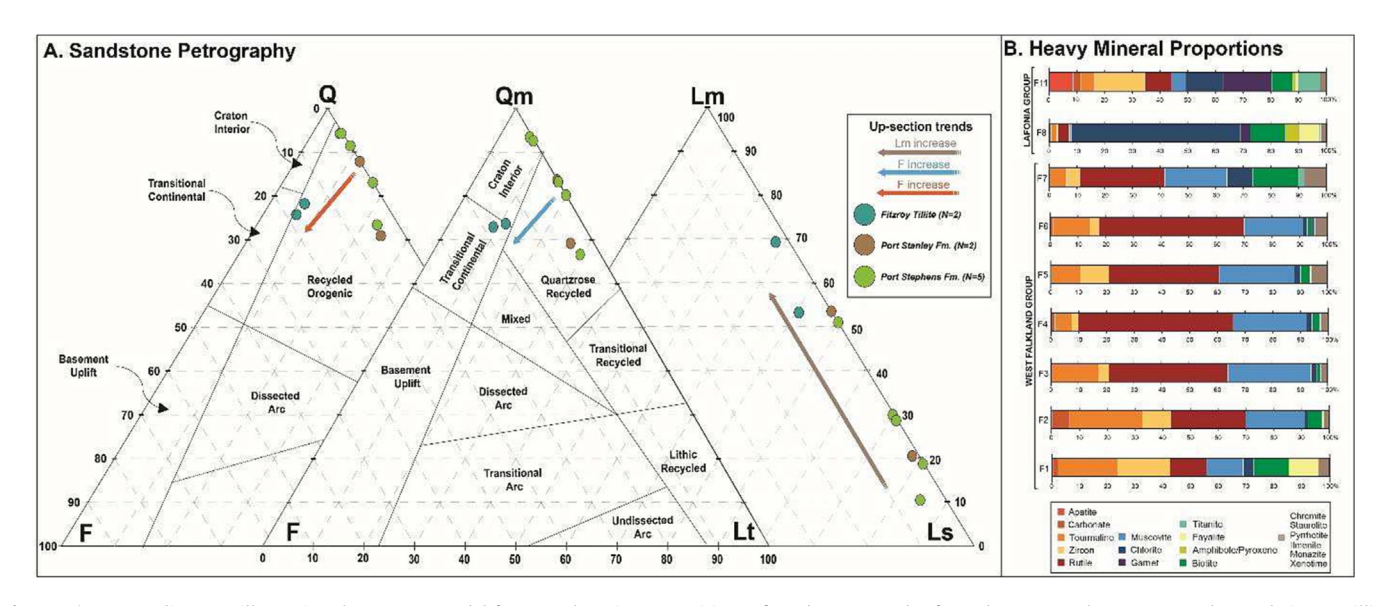


Fig. 7. A.) Ternary diagrams illustrating the average modal framework-grain compositions of sandstone samples from the Port Stephens, Port Stanley, and Fitzroy Tillite formations. Source area characterizations within ternary plots from Dickinson and Suczek (1979); Dickinson et al., (1983). Overall trends in the QFL, QmLtF, and LmLsLV plots denoted by brown (metamorphic lithic), blue (feldspar) and orange (feldspar) arrows. B.) Stacked bar plots illustrating heavy mineral (>2.9 g/cc) assemblages of individual samples from the West Falkland and Lafonia Groups. (For interpretation of the references to color in this figure legend, the reader is referred to the web version of this article.)

muscovite, fayalite, staurolite, monazite, ilmenite, chromite), and (3) ultrastable minerals (zircon, tourmaline, rutile) (Fig. 7b). Samples F1-F6 show high proportions (>55 %) of ultrastable (ZTR) minerals. Sample F7 displays a reduction in ZTR amounts, but an increase in stable and unstable minerals (muscovite, 22.4%; biotite,

9.4%; chlorite, 9.4%). Carboniferous sample F10 exhibits the first upsection shift in heavy mineral proportions with a drastic increase in chlorite (61.2%) and minor increases in amphibole/pyroxene (5%), fayalite (7.2%) and garnet (3.6%). A second upsection shift in Permian sample F11, shows a wide array of heavy mineral

assemblages with the main constituents being zircon (18.3%), garnet (17.8%), and chlorite (13.4%).

4.4. Statistical analysis of U-Pb age spectra

U-Pb detrital zircon age distributions from the F/MI were compared quantitatively with detrital zircon results from the San Rafael Basin, Ventania System (Ramos et al., 2014), Patagonia (Castillo et al., 2016), Tepuel-Genoa Basin (Griffis et al., 2019), Cape Fold Belt (Fourie et al., 2011; Vorster et al., 2021), Karoo Basin (Nxumalo, 2012; Vigietti et al., 2018; Craddock et al., 2019), Antarctic Peninsula (Castillo et al., 2016), and Ellsworth Mountains (Elliot et al. 2016; Craddock et al., 2017; Castillo et al., 2017). Three independent statistical approaches were used as a basis to evaluate the similarity among U-Pb age distributions: (1) multi-dimensional scaling (MDS); (2) K-S test; and (3) '1-0' test.

4.4.1. Multi-dimensional scaling (MDS)

Four separate MDS plots were calculated to maximize the functionality of each test by testing the similarity among cotemporaneous detrital zircon age distributions (Fig. 8). The Silurian MDS plot indicates no clear clustering among detrital zircon age distributions from the F/MI, Ventania System, and Cape Fold Belt, however the F/MI age distributions generally indicate closer relationships with each other. The Devonian MDS plot shows samples F6, F7, and IM-50 from the Port Stanley Formation exhibit the closest similarity with the Witteburg Group (Witteburg) or Crashsite Group (HR6; HR37; HAT; HBJ), as indicated by their first and second 'closest neighbors'. The Carboniferous MDS plot displays samples F8-10 from the Fitzroy Tillite mainly cluster with each other or the Dwyka Group (DTC; DTW), however one instance shows F10's second closest neighbor is from the Sauce Grande Formation (SF) in the Ventania System. Lastly, the Permian MDS plot indicates F11

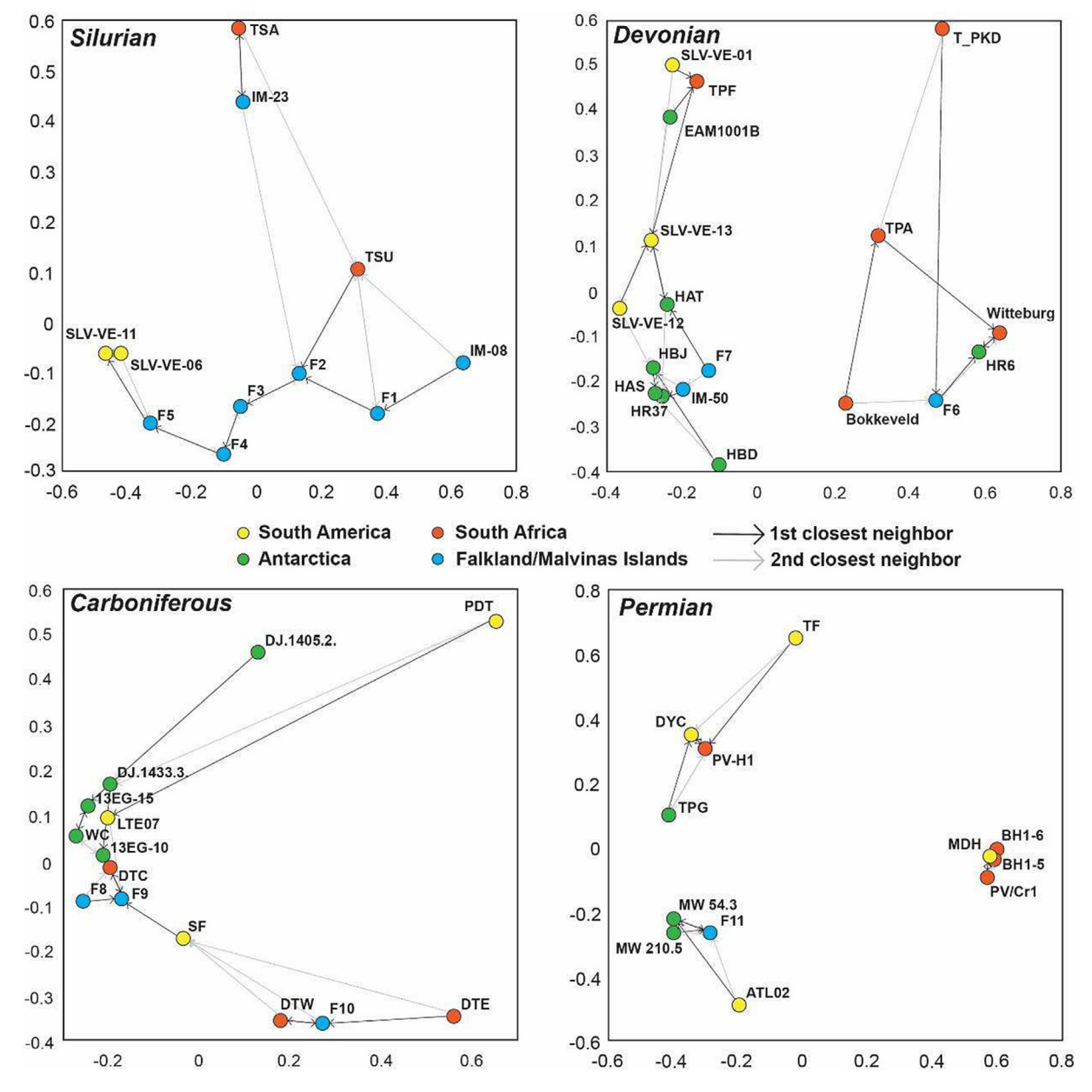


Fig. 8. Multidimensional scaling analysis comparing detrital zircon age distributions among samples from the F/MI (blue), South Africa (orange), Antarctica (green), and South America (yellow). Samples with similar U-Pb age distributions plot closer together and more dissimilar samples plot father apart. Arrows within MDS plots indicate the first (black) and second (grey) closest (most similar) neighbors. (For interpretation of the references to color in this figure legend, the reader is referred to the web version of this article.)

is most similar to MW 54.3 and MW 210.5 from the Polarstar Formation in the Ellsworth Mountains.

4.4.2. Komolgorov-Smirnov test for similarity

Like the MDS approach, four individual K-S tests were performed among cotemporaneous detrital zircon age distributions from the Silurian-Permian, designed to emphasize the statistical relationships between F/MI and adjacent provinces throughout the latter half of the Paleozoic (Fig. 9A). This test generates a 'Pvalue' for each individual similarity tests (summarized in Table 2) and is designed only to evaluate the likelihood that detrital zircon age distributions are not the same (having separate provenance signatures). For the Silurian, similarity tests between the Port Stephens Formation and Napostá and Bravard formations in the Ventania System display the highest percentage of tests with Pvalues < 0.05 (85.71%), while 64.29% of the tests between Table Mountain Group and the F/MI show P-values < 0.05. No Silurian-aged samples from Antarctica were included in this test. Similarly, the Devonian K-S test shows 88.89% of the similarity tests between the Port Stanley Formation and the Ventana Group (Lolén and Providencia formations) resulted in P-values < 0.05. Devonian similarity tests among the F/MI, South Africa (Table Mountain, Bokkeveld, and Witteburg groups) and Antarctica (Crashsite Group) display percentages of 80.00% and 61.90%, respectively. The Carboniferous K-S tests between the Fitzroy Tillite and Dwyka Group show the highest percentage of Pvalues < 0.05 (77.78%), while the similarity tests among the F/MI, South America (Tepuel Group, and Sauce Grande Formation) and Antarctica (Whiteout Conglomerate) show percentages of 44.44% and 33.33%, respectively. The Permian K-S test between the Brenton Loch Formation and coeval Permian strata across southwestern Gondwana show no statistical similarity.

4.4.3. Comparison between confidence intervals of U-Pb detrital zircon age distributions

The third statistical test utilized in this study uses the degree of overlap of 95% confidence intervals between two cumulative distribution functions (Fig. 9B). This test generates a '1-O' value, which categorizes the amount of overlap into three separate categories: low, high, and complete (summarized in Table 3). Like the other two statistical approaches, this test was performed four separate times in order to observe the temporal shifts in similarity among detrital zircon age distributions.

For the Port Stephens Formation, the '1-O' test shows the most 'complete overlaps' occur with the Table Mountain Group (64.3%) and the most 'low overlaps' with the Ventana Group (50%). Similarly, the Port Stanley Formation indicate the most 'high overlap' between the Table Mountain Group (66.7%) and the most 'low overlap' with the Ventana Group (44.4%). The Fitzroy Tillite exhibits the most amount of 'complete overlaps' with the Whiteout Conglomerate, and the most 'low overlaps' with the Dwyka Group. The Brenton Loch Formation displays complete overlap with the ATLO2 (Cochico Group) and PV-H1 (Beaufort Group) but shows little to no overlap with other Permian strata.

While no statistical test indicates a simple, single solution, a few important relationships are present across each of the tests. The Silurian-Devonian MDS plots display the most similarity among the West Falkland Group, Cape Fold Belt, Witteburg Group, and Crashsite Group, with relatively little to no clustering occurring with South American sediments. A similar relationship is observed with the Silurian-Devonian K-S and '1-O' tests, indicated by the high percentages of P-values < 0.05 between the West Falkland Group and Ventana Group, suggesting these groups have a high probability (95%) of having a separate provenance. The relationship between the Fitzroy Tillite and Dwyka Group is difficult to reconcile because these groups plot relatively close together in

MDS space but display poor similarity and low overlap in the K-S and '1-O' tests. Lastly, the Brenton Loch Formation detrital zircon age distribution appears entirely unique from other Permian strata across southwestern Gondwana, but if anything, exhibits the most similarity with the Polarstar Formation the northern Ellsworth Mountains. It is important to note that each of these statistical approaches do not intend to pinpoint exact sediment sources. Instead, these approaches are combined to evaluate the relationship of U-Pb age distributions within different sediment depositories across SW Gondwana, which we interpret to provide insight into the paleo-position of the F/MI.

5. Discussion

To characterize the Paleozoic tectonic setting and sediment sources for the F/MI, we integrate results from U-Pb geochronologic, hafnium isotopic, sandstone petrographic and heavy mineral compositional analyses. We also synthesize published data from geochronological studies of the Paleozoic sections exposed in the Cape Fold Belt, Karoo Basin, Sierra de la Ventana, Ellsworth Mountains, and Antarctic Peninsula to constrain the paleogeographic position of the F/MI during the Paleozoic.

5.1. Provenance and sediment transport

5.1.1. West Falkland Group

Two scenarios of sediment sourcing and transport are evaluated for the Port Stephens and Port Stanley formations: (1) direct derivation from crystalline basement sources or (2) erosion of sedimentary units.

Detrital zircon ages throughout the Silurian-Devonian WFG record a temporally consistent bimodal age distribution (Mesoproterozoic and Neoproterozoic-Cambrian age peaks). If Mesoproterozoic and Neoproterozoic-Cambrian age peaks represent direct contribution from crystalline sources, multiple source regions with overlapping ages can be considered for southern Africa. The Namagua-Natal Metamorphic Complex (NNMC; 2050–1020 Ma) and its corresponding sub-provinces (Keimoes Suite [1150-1100 Ma], Koras Group [1170–1100 Ma], Koperberg and Spektakel Suite [1040–1020 Ma]) were a single extensive structure that likely sourced much of the Mesoproterozoic to late Paleoproterozoic-age detritus. The paucity of Late Proterozoic-Archean zircons in the WFG could have resulted from the NNMC acting as a topographical high (Fourie et al., 2011) between the Kaapvaal Craton and F/MI-Cape Basin. The Bárué Group, Irumide Belt, Unango and Maruppa and Nampula Complexes present within the Mozambique Belt record a Pan-African overprint over Mesoproterozoic crust (Bingen et al., 2009; De Waele et al., 2003, 2006; Kröner, 2001; Kröner et al., 2001), providing an orogen sourcing 1100-950 Ma and 600-550 Ma zircons. The Maud Belt sits adjacent to the Mozambique Belt on the eastern side of the Weddell Sea in Antarctica and is characterized by Mesoproterozoic (1.2-1.0 Ga) supracrustal and intrusive suits intruded by Neoproterozoic-Cambrian granitoids (Bauer et al., 2003; Bisnath et al., 2006; Jacobs et al., 1998, 2003). The eastern boundary of South America hosts the Pan-African Dom Feliciano Belt (~843-570 Ma; Basei et al., 2000; Gaucher et al., 2003; Hartmann et al., 2002; Oyhantçabal et al., 2009), which Rapela et al. (2007) interpret as a principal sediment source for the Balcarce Formation in the Tandilia system of eastern Argentina.

Age-equivalent strata in the Tandilia and Ventania systems and Cape Fold Belt record similar detrital zircon age distributions and SW-directed paleocurrents (prior to microplate rotation) as the Port Stephens and Port Stanley formations (Cingolani and Varela, 1976; Scasso and Mendía, 1985; Hiller and Taylor, 1992; Storey

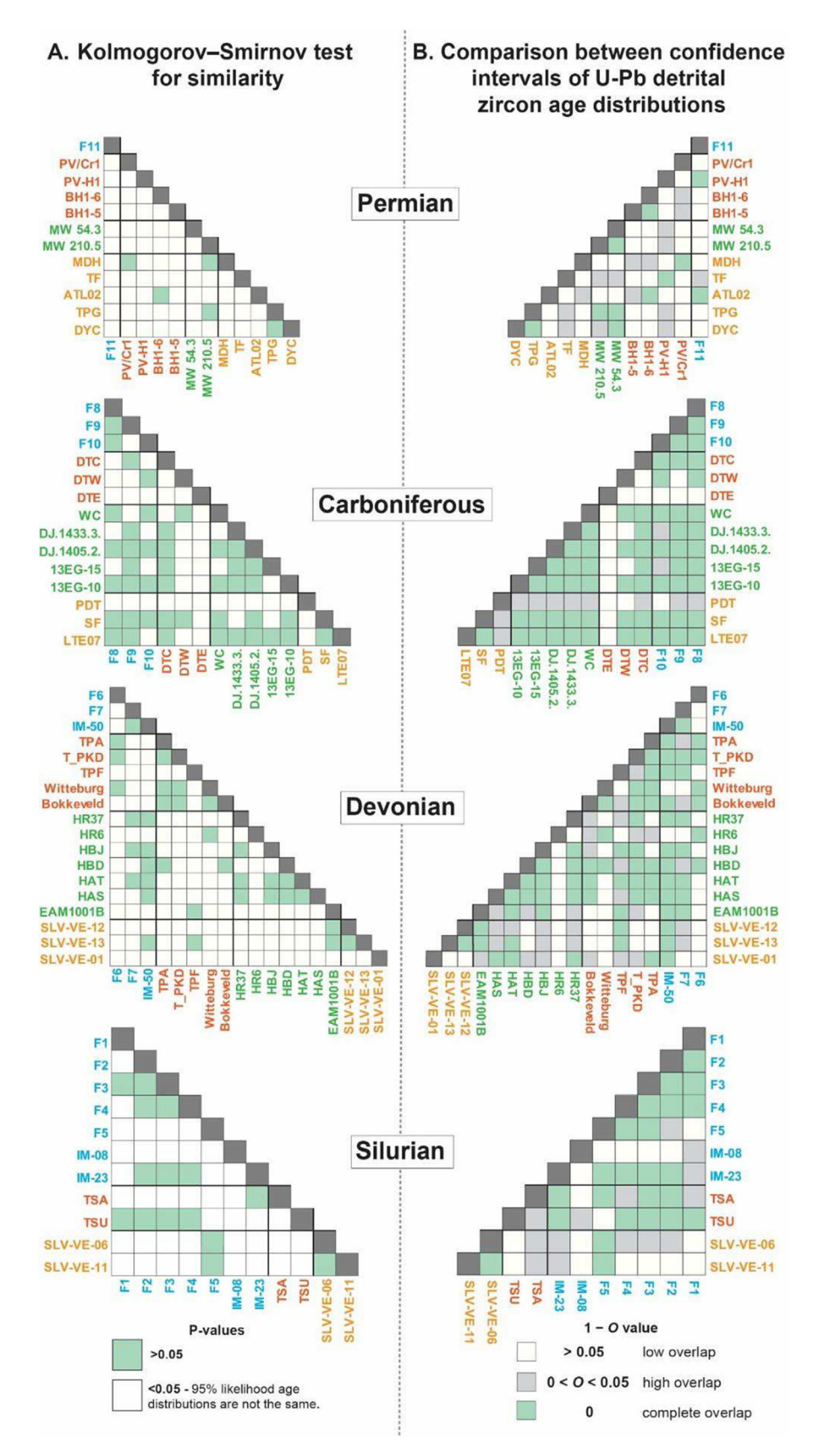


Fig. 9. A.) Cross-plot of K-S P values between samples analyzed in this study and other studies. P-values > 0.0.05 (light green box) indicate samples are not statistically distinguishable as having separate provenance signatures. P-Values < 0.05 (white box) signify that two samples have a 95% likelihood of being statistically distinguishable, meaning they have separate provenance signatures. B.) Cross-plot of '1-O' values between samples analyzed in this study and other studies. Sample comparisons where '0 = 1', or '1 - O = 0', indicate complete overlap (light green box). For this study, O values between 0 and 0.05 are classified as 'high overlap' (gray box). Sample comparisons with '1-O' values > 0.05 are labeled as 'low overlap' (white box). Samples are color coded by F/MI (blue), South Africa (orange), Antarctica (green), and South America (yellow). (For interpretation of the references to color in this figure legend, the reader is referred to the web version of this article.)

Table 2Summary of K-S test results pertinent to the F/MI.

Silurian							
Percentage of K-S Tests with	-P-values > 0.05	Percentage of K-S Tests with -	Percentage of K-S Tests with -P-values < 0.05				
	F/MI		F/MI				
F/MI	33.33%	F/MI	66.67%				
South Africa	35.71%	South Africa	64.29%				
Antarctica	0.00%	Antarctica					
South America	14.29%	South America	85.71%				
	Devo	nian					
Percentage of K-S Tests with	-P-values > 0.05	Percentage of K-S Tests with -	Percentage of K-S Tests with -P-values < 0.05				
-	F/MI	-	F/MI				
F/MI	33.33%	F/MI	66.67%				
South Africa	20.00%	South Africa	80.00%				
Antarctica	38.10%	Antarctica	61.90%				
South America	11.11%	South America	88.89%				
	Carbon	iferous					
Percentage of K-S Tests with	-P-values > 0.05	Percentage of K-S Tests with -	Percentage of K-S Tests with -P-values < 0.05				
	F/MI		F/MI				
F/MI	66.67%	F/MI	33.33%				
South Africa	22.22%	South Africa	77.78%				
Antarctica	66.67%	Antarctica	33.33%				
South America	55.56%	South America	44.44%				
	Perr	nian					
Percentage of K-S Tests with	-P-values > 0.05	Percentage of K-S Tests with -	Percentage of K-S Tests with -P-values < 0.05				
	F/MI		F/MI				
F/MI	0.00%	F/MI	100.00				
South Africa	0.00%	South Africa	100.00				
Antarctica	0.00%	Antarctica	100.00				
South America	0.00%	South America	100.00				

Table 3
Summary of '1-O' test results pertinent to the F/MI.

		Silurian			
Percentage of '1-O' values > 0.05		Percentage of '1-O' values 0 < 0 < 0.05		Percentage of '1-O' values = 0	
	F/MI		F/MI		F/MI
F/MI	28.6%	F/MI	14.3%	F/MI	57.1%
South Africa	14.3%	South Africa	21.4%	South Africa	64.3%
Antarctica	0.0%	Antarctica	0.0%	Antarctica	0.0%
South America	50.0%	South America	35.7%	South America	14.3%
		Devonian	ı		
Percentage of '1-0' values > 0.05		Percentage of '1-O' values 0 < O < 0.05		Percentage of '1-O' values = 0	
	F/MI		F/MI		F/MI
F/MI	66.7%	F/MI	0.0%	F/MI	33.3%
South Africa	20.0%	South Africa	13.3%	South Africa	66.7%
Antarctica	33.3%	Antarctica	4.8%	Antarctica	61.9%
South America	44.4%	South America	22.2%	South America	33.3%
		Carbonifero	ous		
Percentage of '1-O' values > 0.05		Percentage of '1-O' values		Percentage of '1-0' values = 0	
		0 < 0 < 0.05			
	F/MI		F/MI		F/MI
F/MI	0.0%	F/MI	0.0%	F/MI	100.09
South Africa	44.4%	South Africa	0.0%	South Africa	55.6%
Antarctica	0.0%	Antarctica	13.3%	Antarctica	86.7%
South America	11.1%	South America	22.2%	South America	66.7%
		Permian			
Percentage of '1-O' values > 0.05		Percentage of '1-O' values 0 < O < 0.05		Percentage of '1-0' values = 0	
	F/MI		F/MI		F/MI
F/MI	0.0%	F/MI	0.0%	F/MI	0.0%
South Africa	75.0%	South Africa	0.0%	South Africa	25.0%
Antarctica	100.0%	Antarctica	0.0%	Antarctica	0.0%
South America	50.0%	South America	25.0%	South America	25.0%

et al., 1999; Hunter and Lomas, 2003; Ramos et al., 2014; Vorster et al., 2021). However, each of the statistical tests on U-Pb age distributions exhibit little to no similarity between sediments in South America and the F/MI (Figs. 8 and 9).

The other option to consider involves erosion of older sedimentary successions. Pairing detrital zircon U-Pb geochronology, Lu-Hf isotopic signatures, heavy mineral assemblages, and sandstone petrographic data has proved an effective approach in discriminating provenance and sedimentary recycling (Horton et al., 2004; Flowerdew et al., 2007; Garzanti et al., 2007; Bradshaw et al., 2012; Nie et al., 2012; Bush et al., 2016; Vorster et al., 2021). Sandstone petrographic and heavy mineral results from the WFG indicate high proportions of quartz and ultra-stable ZTR proportions (Fig. 7), indicative of either (1) far transport from distal cratonic sources, (2) intense chemical weathering, or (3) derivation from recycled material (Morton and Hallsworth, 1994; 1999; Pettijohn, 1975). It is difficult to discern which option or combination of the three options explains the high ZTR indices, however these results can be compared with results obtained from coeval strata in southern Africa to better characterize sediment sources.

The ε Hf(t) values range between -5.8–15.9 for the WFG, which exhibit similar ranges as time-correlative units within the Crashsite and Trinity Peninsula groups in West Antarctica (Fig. 6). Vorster et al. (2021) suggest the wide array of EHf(t) values (up to \sim 40 epsilon units) within coeval strata in the Table Mountain Group argues against a direct source-to-sink relationship, as each cycle of erosion and deposition would distribute a wider range of ε Hf(t) values from recycled sedimentary units and newly emergent sources. Recent work from Andersen et al. (2016a, 2018b) proposed the erosion of Neoproterozoic-Cambrian sedimentary units within the Gariep, Saldania and Damara belts as the major source for the Paleozoic Cape and Karoo supergroups (Andersen et al., 2018b; Basei et al., 2005; Frimmel et al., 2013; Vorster et al., 2021). The high proportions of quartz fragments and ZTR indices align with the interpretation of a stable cratonic source for the Port Stephens Formation (Aldiss and Edwards, 1999), but similarities in U-Pb age distributions between the WFG and Table Mountain, Witteburg, and Bokkeveld groups potentially suggest the recycling of Neoproterozoic-Cambrian strata (Nama, Port Nolloth, Oranjemund, Boland groups). The range of EHf values for the Port Stephens and Port Stanley formations is far less than the range of EHf values (roughly \sim 20 epsilon units) presented for the Table Mountain Group, possibly suggesting the F/MI received sediment from source regions with reduced geologic diversity (possibly due to smaller drainage systems) or with less recycled clastic material. Therefore, for the WFG, we interpret the Namaqua-Natal Province, and Mozambique and Maud belts as primary basement sources for the Port Stephens and Port Stanley formations, and the Neoproterozoic-Cambrian succession as a minor contributor. This interpretation accords with the S-SW paleocurrents for the WFG (after 180° CW rotation of the Falkland microplate) and supports previous interpretations of a stable cratonic source of sediment to the F/MI passive margin during the Silurian-Devonian (Figs. 10 and 11).

5.1.2. Lafonia Group

The Lafonia Group records two significant changes in provenance, likely resulting from the changing tectonic and climatic regimes in the late Paleozoic. The first provenance change involved an influx of Archean-Mesoproterozoic zircon ages, as recorded in the Carboniferous Fitzroy Tillite. Unlike the abundance of Pan-African orogenic provinces throughout SW Gondwana, Proterozoic-Archean sources are scarcer, and allow for a more robust provenance characterization. The presence of exotic archaeocyathid-bearing limestone clasts within the Fitzroy Tillite led Stone and Thomson (2005) to initially propose the Transantarc-

tic Mountains as a potential sediment source during the late Paleozoic Ice Age (Isbell et al., 2012; Montañez et al., 2016; Griffis et al., 2019; López-Gamundí et al., 2021). Later work from Stone et al. (2012) supported the idea of a Transantarctic and/or Ellsworth Mountains source for the Fitzroy Tillite archaeocyaths, although the discovery of similar archaeocyath limestone clasts in Cambro-Ordovician metaconglomerates in Argentina introduces uncertainty that devalues their use as provenance indicators, unless they are allochthonous (González et al. 2013). Heavy mineral and sandstone petrographic results from the Fitzroy Tillite show high proportions of chlorite, garnet, biotite, and metamorphic lithic fragments (Fig. 7), suggesting greater contribution from metamorphic terranes (Dickinson and Suczek, 1979; Dickinson et al., 1983). U-Pb age distributions from the Fitzroy Tillite display a considerable amount of Paleoproterozoic 1.72-1.77 and 1.65-1.6 Ga and Archean 3.1-2.5 Ga zircon grains, suggestive of a Transantarctic source. The Nimrod Complex, located in the central Transantarctic Mountains, underwent major crustal reworking at 2.5 and 1.7 Ga during the genesis of the East Antarctic shield and associated Paleoproterozoic amalgamation of the Nuna supercontinent (Goodge et al., 2001; Goodge and Fanning, 2016). Gneiss, ecoligitic and meta-igneous rocks within the Nimrod Complex document a phase of deep-crustal metamorphism, thickening and magmatism at 1730-1700 Ma, known as the Nimrod Orogeny (Goodge and Fanning, 2016). Paleoproterozoic-Archean terranes (Stratton Group) located within the Shackleton Range (northern Transantarctic Mountains) yield zircons with core ages of \sim 2520 Ma and magmatic/metamorphic rims of \sim 1740 Ma (Will et al., 2009; Riley et al., 2020). Aside from the Transantarctic Mountains, other Paleoproterozoic and Archean source terranes include the Kaapvaal (southern Africa) and Rio de la Plata (South America) cratons. A similarly low proportion of Archean to Paleoproterozoic zircon age modes is noted for Rocha, Oranjemund, and Natal groups (southern Africa), and Providencia Formation (Tandilia Region, South America) despite their close proximity to their respective Archean cratons (Fourie et al., 2011; Uriz et al., 2011; Andersen et al., 2016a; Kristoffersen et al., 2016). These cratonic rocks were likely covered until they were exhumed during the Carboniferous Gondwana glaciation (Andersen et al., 2016b).

Statistical comparisons among the Fitzroy Tillite, Whiteout Conglomerate (Ellsworth Mountains), Dwyka Group (Karoo Basin), and Sauce Grande Formation present varied results. MDS results indicate clustering among F/MI samples (F8, F9 and F10) and the Dwyka Group (DTC, DTW) and Sauce Grande Formation (SF). Perhaps the most dissimilarity within the MDS plots occurs among the Lafonia Group (Fitzroy Tillite and Brenton Loch Formation) and coeval strata of the Tepuel-Genoa, San Rafael, and Hespérides basins in South America (Figs. 8-9). We observe diminished similarity from east to west, which is consistent with the prerotation westward glacial paleo-ice flow during deposition of the Fitzroy Tillite (Frakes and Crowell, 1967). Given the scarce populations of Archean-Proterozoic age grains, the archaocyath limestone clasts, and the metamorphic lithics present within the Fitzroy Tillite, we interpret either the Nimrod Complex and/or Shackleton Range to have contributed sediment to the Fitzroy Tillite. The Ellsworth Ice Sheet, originating within the central Transantarctic Mountains, flowed westward and likely transported detritus to the regions encompassing the EWM, F/MI, and eventually western Argentina. This hypothesis is also supported by the diminishing proportions of pyrope garnets from east to west (Craddock et al., 2017; 2019), which were sourced in the Ellsworth ice center and Transantarctic Mountains. The discrepancies noted between the Fitzroy Tillite and Dwyka Group zircon age distributions are likely linked to derivation from separate ice sheets, the Ellsworth and Dwyka ice sheet, respectively (Fig. 12), although the presence of archaeocyath-limestone clasts probably derived from the

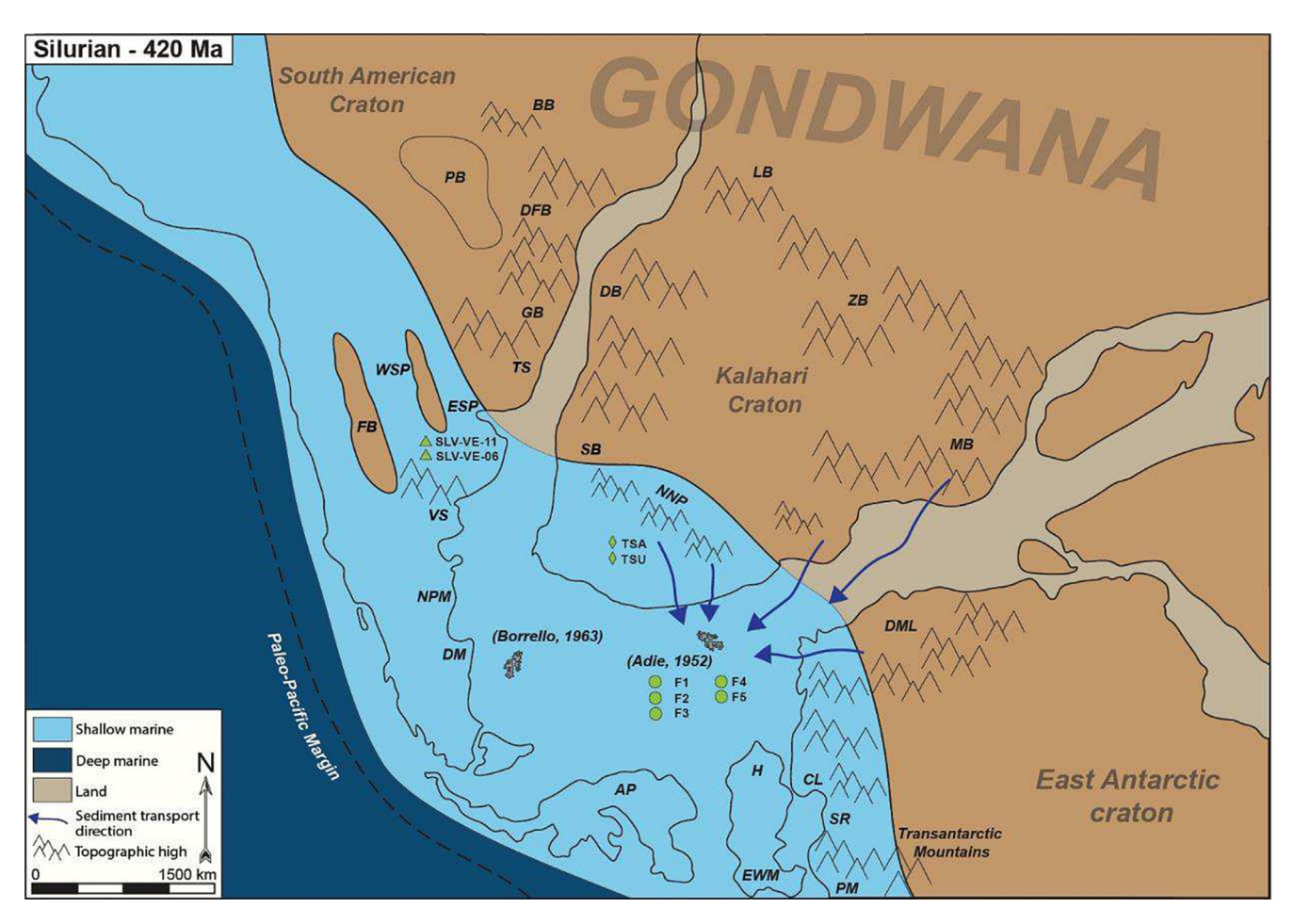


Fig. 10. Paleogeographic reconstruction at ~420 Ma with arrows representing likely sediment pathways for the Port Stephens Formation. Blue arrows indicate deposition via fluvial pathways shedding primarily off topographic highs within the Saldania Belt, Namaqua-Natal Province, Mozambique Belt, Coats Range, and overlying Paleozoic-Neoproterozoic sedimentary cover. Dashed line represents the nascent Paleo-Pacific Margin. Physical features: AP, Antarctic Peninsula; BB, Brazilia Belt; CL, Coats Land; DB, Damara Belt; DFB; DM, Deseado Massif; DFB, Dom Felicio Belt; DML, Dronning Maud Land; EWM, Ellsworth Whitmore Mountains; ESP, Eastern Sierras Pampeanas; FB, Famatinia Belt; GB, Gariep Belt; H, Haag Nunatak; LB, Lufilian Belt; MB, Mozambique Belt; NNP, Namaqua-Natal Province; NPM, North Patagonian Massif; PB, Parana-panema block; PM, Pensacola Mountains; SB, Saldania Belt; SR, Shackleton Range; TS, Tandilia System; VS, Ventania System; WSP, Western Sierras Pampeanas; ZB, Zambezi Belt. Plate reconstructions taken from Gplates PALEOMAP global paleogeography software available online at https://www.gplates.org/. (For interpretation of the references to color in this figure legend, the reader is referred to the web version of this article.)

Transantarctic Mountains in Dwyka Group diamictites perhaps indicate some alternation of the two ice streams with the potential for reworking and mixing of their deposits.

The second shift in provenance within the Lafonia Group is recorded by the U-Pb, Lu-Hf, and heavy mineral data for the Brenton Loch Formation (F11). By late Carboniferous-early Permian time, subduction along the Gondwanan margin initiated an extensive magmatic arc that generated the granitoids and orthogneisses present throughout eastern Marie Byrd Land, Thurston Island, Antarctic Peninsula, and southern South America (Elliot, 2013; Riley et al., 2012; Eliot et al., 2016; Gianni and Navarret, 2022). The Brenton Loch Formation exhibits detrital zircon age peaks at \sim 269 Ma, \sim 336 Ma, \sim 536 Ma, \sim 851 Ma, and \sim 1020 Ma. The youngest single zircon age reported here is 255.8 +/- 2.8 Ma, and the appearance of thirty-five zircons between the ages 286.8-256 Ma confirms the inception of a magmatic arc contributing sediment to the F/MI succession. Carboniferous-Permian zircons also appear in the coeval strata within the Karoo Basin (Balfour, Teekloof, and Vryheid formations; Nxumalo, 2012; Viglietti et al., 2018), Ellsworth Mountains (Polarstar Formation; Elliot et al., 2016), Ventania System (Tunas Formation, Ramos et al., 2014), Tepuel-Genoa Basin (Mojón de Hierro Fm.), Antarctic Peninsula

(Trinity Peninsula Group: Castillo et al., 2016) and southern Patagonia (Duque de York Complex; Castillo et al., 2016). Permian MDS results indicate clustering among three sectors (Fig. 8), with the Brenton Loch Formation (F11) exhibiting the closest similarity with the Polarstar Formation (MW 54.3 and 210.5) in the Ellsworth Mountains. An opposite relationship is observed in the K-S and '1-0' tests, which show little to no similarity between the Brenton Loch Formation and coeval Permian strata across SW Gondwana (Fig. 9). Thus, we support the interpretation from Elliot et al. (2016) that argues for two separate sub-basins, or a distinct unconnected basin, between the F/MI and Ellsworth Mountains during the Permian. The diminished Neoproterozoic-Cambrian and Mesoproterozoic age proportions suggest that the Precambrian orogenic regions contributing the bulk of sediments to the WFG were minor contributors during the Permian; rather, the active magmatic arc along the Paleo-Pacific margin was the principal sediment source for the Brenton Loch Formation. It is likely the 280-250 Ma zircons were delivered to the F/MI from the magmatic arc along the Paleo-Pacific margin; unroofing of the older, mid-Paleozoic magmatic arc and Carboniferous-Ordovician strata during Gondwanide tectonism likely provided the minor 490-330 Ma zircon age group within the Brenton Loch Formation (Fig. 13)

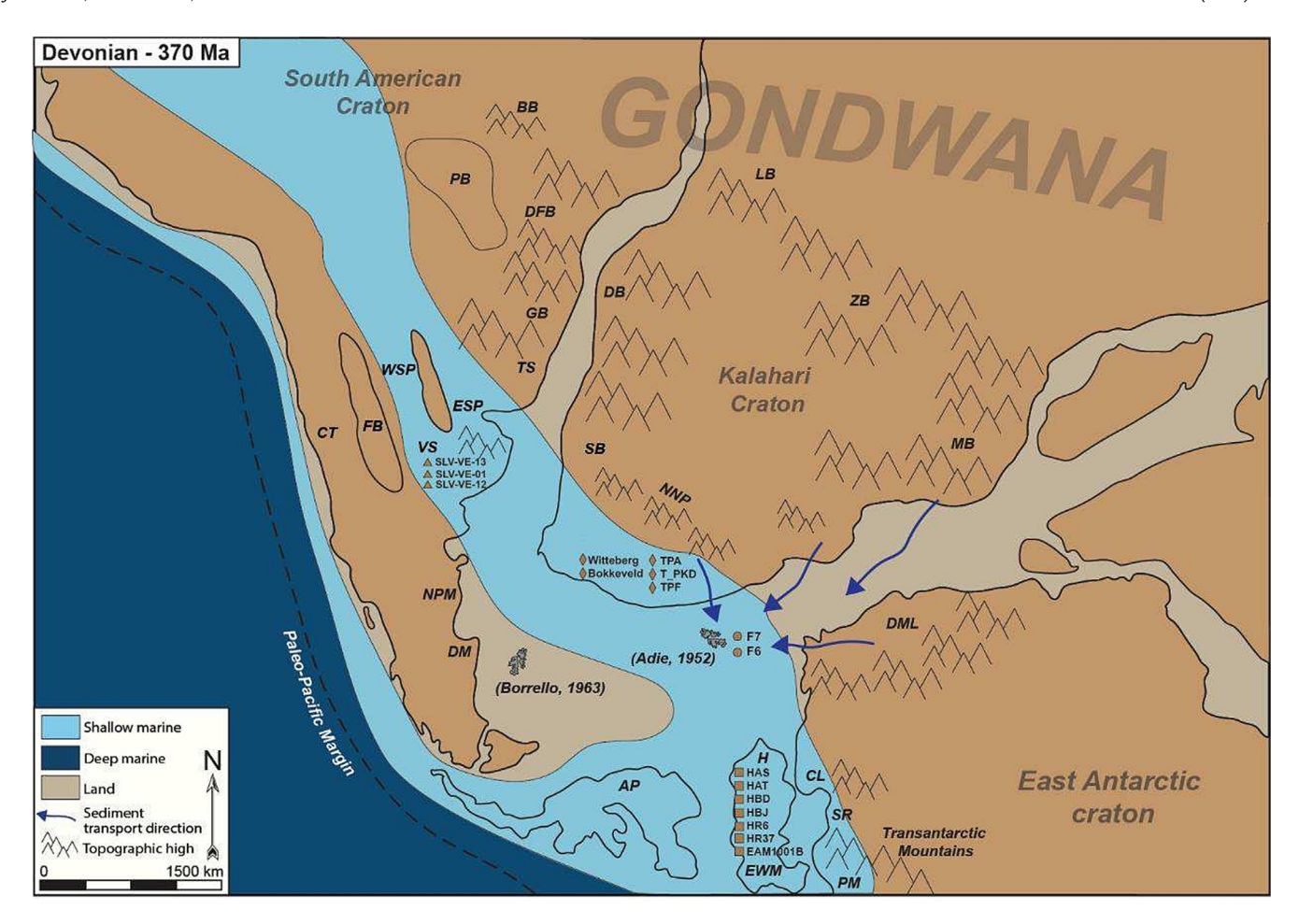


Fig. 11. Paleogeographic reconstruction at ~380 Ma with arrows representing likely sediment pathways for the Port Stanley Formation. Blue arrows indicate deposition via fluvial pathways shedding off topographic highs within the Saldania Belt, Namaqua-Natal Province, Mozambique Belt, Coats Range, and overlying Paleozoic-Neoproterozoic sedimentary cover. Plate reconstructions taken from Gplates PALEOMAP global paleogeography software available online at https://www.gplates.org/. (For interpretation of the references to color in this figure legend, the reader is referred to the web version of this article.)

5.2. Paleogeographic position during the Paleozoic

Adie (1952) suggested the F/MI were situated within a microcontinental block that rotated 120° CW about a vertical axis during transform-related breakup of Gondwana. Later studies supported his interpretation of the F/MI as an eastern extension to the N-verging Cape Fold Belt, and thus a missing SE continuation of the Karoo Basin (Mitchell et al., 1986; Marshall, 1994; Mussett and Taylor, 1994; Curtis and Hyam, 1998; Thistlewood and Randall, 1998; Thomson, 1998; Trewin et al. 2002; Stone, 2016). A suggested refinement of the location for the F/MI presented by Stanca et al. (2019, 2022), based on the amount of extension and microcontinental block rotation in strike-slip systems, placed the archipelago ~ 250 km SW of the Adie's proposal, aligning with the trend of the Cape Fold Belt at Port Elizabeth.

Several studies have reported U-Pb ages of detrital zircons for selected Paleozoic units within the F/MI and used these to aid reconstruction of the paleo-position of the islands (Ramos et al., 2017; Craddock et al., 2019; Vorster et al., 2021). Ramos et al. (2017) and Vorster et al. (2021) highlight the similar late Mesoproterozoic to Neoproterozoic ages between the WFG and those of the Natal Group (Vorster et al., 2016), but argue those same ages also reflect derivation from granitoids and metasedimentary units in southern South America (Patagonia). These conclusions were taken as support for the Borrello (1963) hypothesis of the F/MI as a fixed promontory of the South American mainland since the Paleozoic. When comparing statistical tests for F/MI detrital zircon ages with

those in South America, southern Africa, and Antarctica, there is a significant difference between the age populations in South America and F/MI; by default, this would favor a South Africa-Antarctica connection for the microplate containing the F/MI.

Statistical analysis of the Port Stephens and Port Stanley formations detrital zircon age distributions show the most similarity with the Table Mountain and Crashsite groups but diverge from the age distributions of the Ventana Group. Similar relationships are observed within the Carboniferous age distributions, which display slight similarity between the Fitzroy Tillite and Dwyka Group, and slightly lower similarity with the Whiteout Conglomerate.

Therefore, we interpret the WFG to have greater affinity with South Africa and EWM, and the Fitzroy Tillite to have primary sources in the Transantarctic Mountains. The transition from a passive margin to a foreland basin was accompanied by deformation associated with the Gondwanide Orogeny (recorded within the Sierra de la Ventana of Argentina, the Cape Fold Belt, F/MI, the Ellsworth Mountains, and the Pensacola Mountains), and may have segregated depositional systems and sediment routing patterns that had been connected since at least the Silurian.

5.3. Tectonic implications

The WFG and equivalent clastic sequences exposed throughout southwestern Gondwana were deposited within a passive margin that opened in the early to mid-Paleozoic (Ramos and Naipauer,

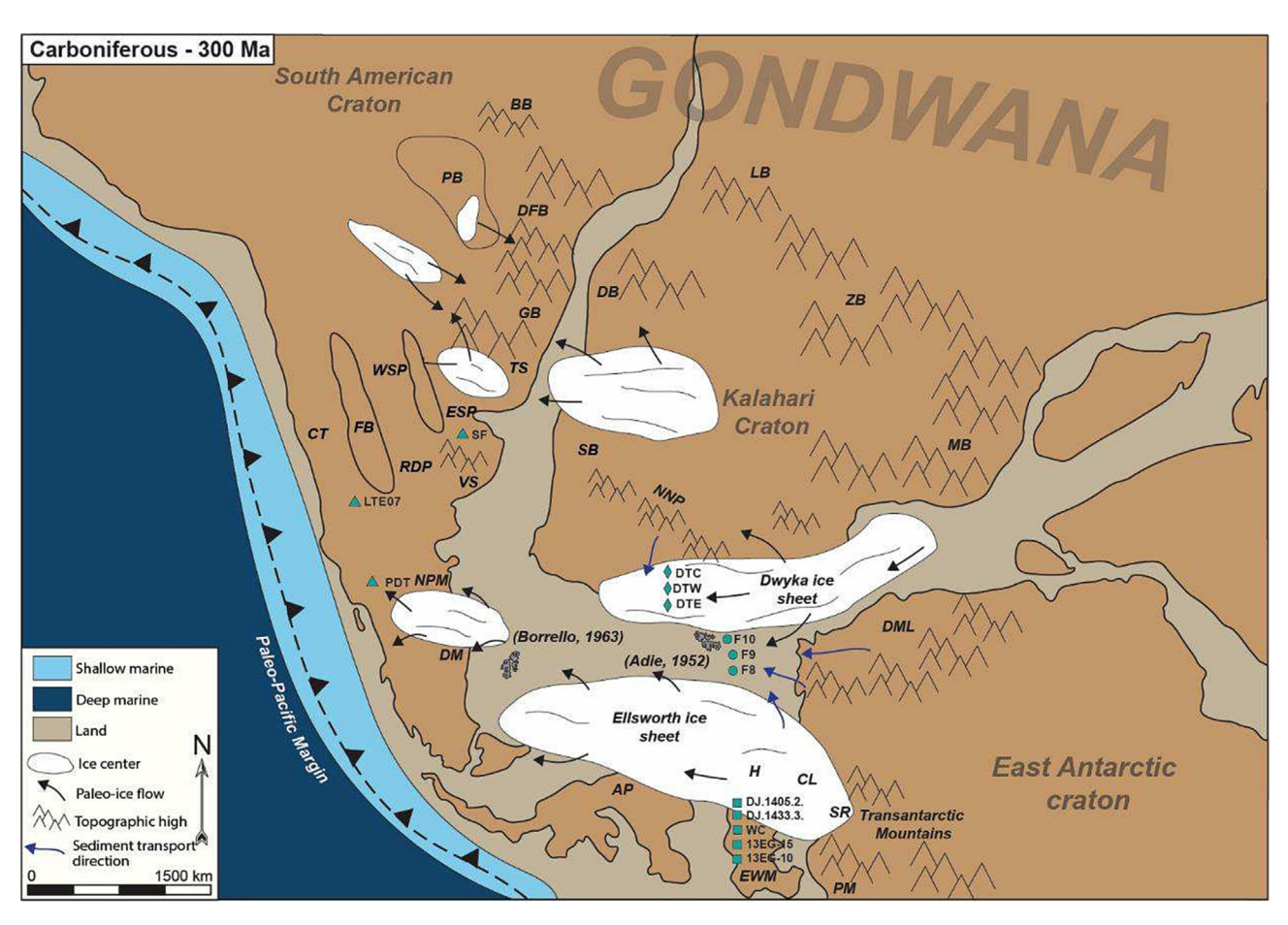


Fig. 12. Paleogeographic reconstruction at ~300 Ma during the LPIA. Multiple diachronous glaciations (colored in white) throughout the Carboniferous influenced sediment transport across the region (Isbell et al., 2012; Craddock et al., 2019). Overall westward ice center movement (small black arrows) likely facilitated sediment transport from Transantarctic sources to the Falkland-Malvinas Islands during deposition of the Fitzroy Tillite (López-Gamundí, 1997; Visser, 1997a, 1997b; Visser et al., 1997; Rocha-Campos et al., 2008; Isbell et al., 2008). The presence of archaeocyathid clasts (Stone and Thomson, 2005; and Stone et al., 2012), increased proportions in Proterozoic-Archean aged zircon grains and metamorphic lithics in the Fitzroy Tillite also indicate Transantarctic craton margin sources (Miller Range, Shackleton Range, and Pensacola-Theil Mountains).

2014). Aldiss and Edwards (1999) proposed a potential shift in provenance in the WFG's Port Stephens Formation due to the varying heavy mineral content within sandstones. However, we find the WFG exhibited a stable sediment supply from the Mozambique and Maud belts and recycled Neoproterozoic-Cambrian sedimentary successions within southern Africa (Nama, Port Nolloth, Oranjemund, Boland groups). These sediments were delivered to a gently shelving alluvial to coastal plain along a passive margin undergoing long-lived, regional subsidence (Hunter and Lomas, 2003; Vorster et al., 2021). Late Devonian to early Carboniferous (380-320 Ma) magmatic suites present within Patagonia and Antarctic Peninsula indicate the re-establishment of subduction along the Paleo-Pacific margin (Capaldi et al., 2021), but the paucity of syndepositional Silurian-Devonian zircons within the WFG suggest that the F/MI was remote from Patagonia, and was instead linked to a region undergoing magmatic quiescence, likely related to ongoing collisional orogenesis resulting from terrane accretion, prolonged flat slab subduction, or development of a passive or transform margin (Ramos et al., 1984; Sims et al., 1998; Dalziel et al., 2000; Cawood, 2005; Bahlburg et al., 2009; Ramos and Folguera, 2009; Rapalini, 2018; Dahlquist et al., 2018). We interpret the absence of Silurian-Devonian zircons in the WFG, coupled with the predominance of ultra-stable heavy minerals (ZTR) and quartz grains, as indicating deposition along a passive margin. This interpretation aligns with those made for the Table Mountain Group (Vorster et al., 2021) and Crashsite Group (Craddock et al.,

2017), suggesting the F/MI shared a broad depositional environment with southern Africa and the Ellsworth-Whitmore terrane until the Permian, when it was likely segregated into different sub-basins during the transition from a passive margin to a foreland basin.

Like the F/MI, the Ellsworth Whitmore terrane is considered a large, rotated microplate (720,000 km²) with the highest range in Antarctica, the Ellsworth Mountains, and a few widely separated small ranges and nunataks (Dalziel and Elliot, 1982; Dalziel et al., 1987; Grunow et al., 1987; Randall and MacNiocaill, 2004; Storey et al., 1988; Dalziel, 2007). In counterpart to the F/MI microplate, the EWM block appears to have undergone CCW rotation. The EWM exhibit similar stratigraphic, structural, and geochronological relationships observed in the Cape and Karoo supergroups of South Africa, and the West Falkland and Lafonia groups in the F/ MI (Curtis and Storey, 1996). These connections existed until the Permian, when several deformational and magmatic episodes segregated the once continuous passive margin throughout the Silurian-Devonian (Elliot et al., 2016). Several structural studies in the F/MI and Cape Fold Belt identified northward-verging (in restored Gondwana position) deformational episodes between the early Permian to middle Triassic (Hälbich et al., 1983; Gresse et al., 1992; Curtis and Hyam, 1998). Conversely, the EWM experienced two episodes of Permian deformation, both of which are interpreted as eastward-verging (Curtis, 2001). The differences in intensities and direction of deformation between the EWM and

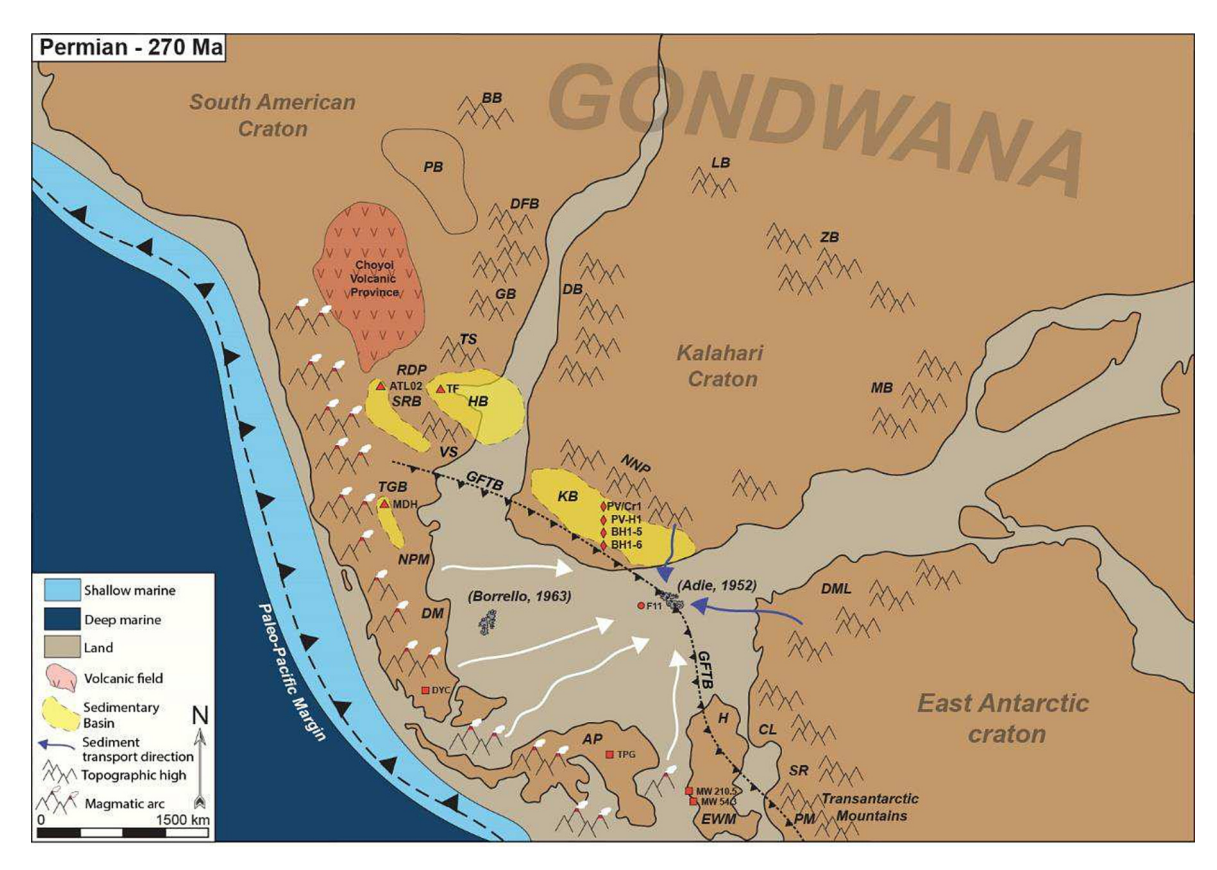


Fig. 13. Paleogeographic reconstruction at ~270 Ma after the onset of the Carboniferous-Permian magmatic arc resulting from subduction related magmatism. The high proportions of late Paleozoic (~270 Ma) detrital zircon grains present within the Brenton Loch Formation and other coeval lithostratigraphic within various basins suggests the magmatic arc along the Paleo-Pacific Margin served as the principal sediment source for the whole region. The subsequent transition into foreland basin encompassed segments of South America, south Africa, Antarctica, and the Falkland-Malvinas Islands. Key features: GFTB; Gondwanide fold-thrust belt; HB, Hesperides Basin; KB, Karoo Basin; RDP, Rio de la Plata Craton; SRB, San Rafael Basin; TGB, Tepuel-Genoa Basin. White arrows indicate deposition via ash from the magmatic arc and blue arrows indicate deposition from fluvial processes. (For interpretation of the references to color in this figure legend, the reader is referred to the web version of this article.)

F/MI suggests the EWM were positioned inboard of the structural front (Curtis, 2001; Elliot et al., 2016). Contrasts in paleocurrents between the F/MI and EWM also indicates separate depositional systems, which show present-day N-NE directed paleocurrents for F/MI Permian strata (derived from the incipient Gondwanide orogen) and westward paleocurrents for the Polarstar Formation (Trewin et al., 2002; Elliot et al., 2016). Coupling the structural and paleocurrent dissimilarities among the CFB, F/MI and EWM supports the idea the Karoo and Lafonia successions were deposited within a different sub-basin, or distinct unconnected basin, from the Ellsworth Mountains, which was likely part of a basin extending from the central Transantarctic Mountains into the proto-Weddell Sea region (Elliot et al., 2016). It should be noted that the mechanism of displacement and rotation of the EWM terrane, like that of the F/MI microplate, is not immediately apparent as it predates the formation of oceanic lithosphere in the Weddell Sea region (Jordan et al., 2016).

The geodynamic setting supporting widespread Permian volcanism along the southwestern Gondwanan margin is not well constrained, leading to two end-member scenarios explaining the onset of Permian volcanism. One scenario involves detachment of the subduction plate caused by horizontal slab tearing (Kay et al., 1989; Pankhurst et al., 2006; Gianni and Navarrete, 2022), while the other suggests continued subduction associated with changes in slab-dip angle (del Rey et al., 2016; Oliveros et al., 2020; Gregori et al., 2020). The \sim 269 Ma age peak and associated 'isotopic pullup' observed in the ϵ Hf(t) values for the Brenton Loch Formation aligns with temporal and geochemical signatures in South America, Antarctic Peninsula, and Thurston Island, all which

represent a continental arc flare-up associated with the Choiyoi Magmatic Province (Nelson and Cottle, 2019). Therefore, even though the Brenton Loch Formation, Trinity Peninsula Group, and Duque de York Complex were not a part of a single, broad depositional system, these units may record the changes in the geodynamic setting of the Choiyoi Magmatic Province.

5.4. Late Paleozoic ice sheet dynamics

By the Carboniferous, three principal glacial intervals (late Devonian (Famennian), middle Mississppian (Visean), late Mississippian (Serpukhovian); Rosa and Isbell, 2021) constituted the longest icehouse interval in the Phanerozoic. Two major ice centers, the Dwyka Ice Sheet and the Ellsworth Ice Sheet, altered sediment transport around southwestern Gondwana. The Dwyka Ice Sheet, responsible for the Dwyka diamictites in the greater Karoo Basin, originated in present-day Zimbabwe and flowed westsouthwest (Craddock et al., 2019). While a preponderance of garnets is found within the Dwyka diamictites, an even greater proportion exists within the Whiteout Conglomerate in the EWM (Craddock et al., 2019), suggesting a more proximal sediment source within the Ellsworth Mountains. The diamictites within the Fitzroy Tillite and Whiteout Conglomerate also contain clasts of Cambrian archaeocyathid limestone, metamorphic lithics/heavy mineral assemblages (chlorite, favalite and biotite), and increased proportions of Paleoproterozoic-Mesoproterozoic zircons, which were all likely sourced from the Ellsworth ice sheet (Fig. 12).

6. Conclusions

The Paleozoic Gondwanan margin between the Sierra de la Ventana and the Ellsworth Mountains encapsulated multiple primary sources and recycled sedimentary strata regions that supplied the two dominant detrital zircon age modes. The overlap in zircon age fractions among the F/MI, South America, Africa, and Antarctica make it difficult to define a specific provenance for the West Falkland and Lafonia groups. However, the synthesis of U-Pb geochronology, Hf-isotopic signatures, sandstone petrography, heavy mineral assemblages, and multiple statistical tests allow for the first robust provenance analysis of samples spanning the Paleozoic stratigraphic succession within the F/MI. The dominant age fractions of Neoproterozoic-Cambrian and Mesoproterozoic zircons are present not only within the WFG, but in coeval strata from South America (Ventana Group), southern Africa (Table Mountain Group), and Antarctica (Crashsite Group). Nevertheless, the utilization of three different statistical tests shows the Port Stephens and Port Stanley formations exhibit the most similarity with the Crashsite and Table Mountain groups. Similarly close relationships are also observed for the Dwyka Group, Fitzroy Tillite, and Whiteout Conglomerate. Contrarily, the Paleozoic stratigraphic succession within the Ventania System exhibits little to no similarity with contemporaneous Paleozoic strata in Africa and Antarctica.

The subtle contrast in detrital zircon age distributions between the Dwyka Group and Fitzroy Tillite suggests the presence of two unique ice centers controlling sediment supply during the Carboniferous. The Ellsworth ice sheet provided the influx of Mesoproterozoic-Paleoproterozoic zircons, archaeocyathidlimestone erratics, pyrope garnet concentrations, and metamorphic lithic fragments from the Transantarctic Mountains during deposition of the Whiteout Conglomerate and Fitzroy Tillite and was able intermittently to introduce archaeocyathid-limestone clasts into the eastern deposits of the Dwyka Group. By the Permian, the principal sediment source to the F/MI succession was the Choiyoi Magmatic Province along the Paleo-Pacific margin, which was supplying clastic and volcaniclastic sediments to the Ventania, Karoo, Ellsworth, and F/MI systems. Each of these regions exhibit strong late Paleozoic zircon age peaks (\sim 280–260 Ma), however, the lack of similarity between their age distributions suggests each was segregated into its own depositional system within the continuous passive margin that occupied the region for much of the Paleozoic. This basin segregation accompanied the Gondwanide orogenesis.

In terms of palaeogeography, our results are most readily accommodated within a Gondwana reconstruction that includes the F/MI as part of a craton-directed fold-thrust belt extending from the Ventania region of Argentina, through the Cape region of South Africa and into the Ellsworth and Pensacola mountains of Antarctica. The position of the F/MI within this assemblage, supported by the closest provenance correlations of the WFG and the Fitzroy Tillite Formation, is between the eastern Cape and the Ellsworth Mountains. This is the Adie (1952) solution to the enigmatic geological relationships of the F/MI. It follows that our results support CW rotation of a F/MI microplate during the initial, early Jurassic break-up of Gondwana as it moved away from South Africa and, as the Atlantic Ocean opened, assumed its current position adjacent to South America.

CRediT authorship contribution statement

J.R. Malone: Conceptualization, Methodology, Formal analysis, Investigation, Resources, Writing – original draft, Writing – review & editing. **I.W.D. Dalziel:** Conceptualization, Investigation, Writing

review & editing, Supervision. P. Stone: Investigation, Writing – review & editing. B.K. Horton: Conceptualization, Methodology, Investigation, Writing – review & editing, Project administration, Funding acquisition.

Declaration of Competing Interest

The authors declare that they have no known competing financial interests or personal relationships that could have appeared to influence the work reported in this paper.

Acknowledgements

Thank you to the Arizona LaserChron Center at the University of Arizona for processing U-Pb geochronology data, ZirChron (Dr. Victor Valencia) for seperating samples for this project, and the Colorado School of Mines Automated Mineralogy Laboratory (Dr. Katharine Pfaff) for processing of heavy mineral data. This research was funded by NSF grant EAR-1918541 awarded to B.K. Horton. A special thank you to Matthew Malkowski for assisting with discussions regarding the statistical analysis. We thank Teal Riley and an anonymous reviewer for their thoughtful reviews that improved this manuscript. Ian Dalziel thanks Captain Chris Kobusch and his sailing companions aboard SV *Pelagic Australis* in Falkland/Malvinas Islands waters in 2019. Phil Stone contributes by permission of the Executive Director, British Geological Survey (UKRI) and thanks the Falkland Islands Department of Mineral Resources for logistical support.

Appendix A. Supplementary material

Supplementary data to this article can be found online at https://doi.org/10.1016/j.gr.2023.04.004.

References

- Adie, R.J., 1952. The position of the Falkland Islands in a reconstruction of Gondwanaland. Geol. Mag. 89, 401–410.
- Alasino, P.H., Dahlquist, J.A., Pankhurst, R.J., Galindo, C., Casquet, C., Rapela, C.W., Larrovere, M.A., Fanning, C.M., 2012. Early Carboniferous sub- to mid-alkaline magmatism in the Eastern Sierras Pampeanas, NW Argentina: A record of crustal growth by the incorporation of mantle-derived material in an extensional setting, Gondwana Res. 22 (3–4), 992–1008. https://doi.org/10.1016/j.gr.2011.12.011.
- Aldiss, D. T. and Edwards, E. J., 1999. The Geology of the Falkland Islands. British Geological Survey Technical Report WC/99/10, Available online at: http://nora.nerc.ac.uk/507542/.
- Allen, J.L., Johnson, C.L., Heumann, M.J., Gooley, J., Gallin, W., 2012. New technology and methodology for assessing sandstone composition: A preliminary case study using a quantitative electron microscope scanner (QEMScan), in Mineralogical and Geochemical Approaches to Provenance. Geological Society of America. https://doi.org/10.1130/2012.2487(11).
- Andersen, T., Elburg, M., Cawthorn-Blazeby, A., 2016a. U-Pb and Lu-Hf zircon data in young sediments reflect sedimentary recycling in eastern South Africa. J. Geol. Soc. 173, 337–351. https://doi.org/10.1144/jgs2015-006.
- Andersen, T., Kristoffersen, M., Elburg, M.A., 2016b. How far can we trust provenance and crustal evolution information from detrital zircons? A south African case study. Gondwana Res. 34, 129–148.
- Andersen, T., Kristoffersen, M., Elburg, M.A., 2018a. Visualizing, interpreting, and comparing detrital zircon age and Hf isotope data in basin analysis a graphical approach. Basin Res. 30, 132–147. https://doi.org/10.1111/bre.12245.
- Andersen, T., Elburg, M.A., van Niekerk, H.S., Ueckermann, H., 2018b. Successive sedimentary recycling regimes in southwestern Gondwana: Evidence from detrital zircons in Neoproterozoic to Cambrian sedimentary rocks in southern Africa. Earth-Sci. Rev. 181, 43–60. https://doi.org/10.1016/j. earscirev.2018.04.001.
- Bahlburg, H., Vervoort, J.D., Du Frane, S.A., Bock, B., Augustsson, C., Reimann, C., 2009. Timing of crust formation and recycling in accretionary orogens: Insights learned from the western margin of South America. Earth-Sci. Rev. 97 (1–4), 215–241. https://doi.org/10.1016/j.earscirev.2009.10.006.
- Basei, M.A.S., Siga Jr., O., Masquelin, H., Harara, O.M., Reis Netto, J., Preciozzi, F., 2000. The Dom Feliciano Belt (Brazil-Uruguay) and its foreland domain, the Rio de la Plata Craton: Framework, tectonic evolution and correlation with similar provinces of Southwestern Africa. In: Cordani, U., Milani, E., Thomaz Filho, A.,

- Campos, D. (Eds.), Tectonic Evolution of South America, 31st International Geological Congress, Rio de Janeiro, Brazil. FINEP, Rio de Janeiro, pp. 311–334.
- Basei, M.A.S., Frimmel, H.E., Nutman, A.P., Preciozzi, F., Jacob, J., 2005. A connection between the Neoproterozoic Dom Feliciano (Brazil/Uruguay) and Gariep (Namibia/ South Africa) orogenic belts - evidence from a reconnaissance provenance study. Precambr. Res. 139, 195–221. https://doi.org/10.1016/j. precamres.2005.06.005.
- Bauer, W., Jacobs, J., Fanning, C.M., Schmidt, R., 2003. Late Mesoproterozoic arc and back-arc volcanism in the heimefrontfjella (East Antarctica) and implications for the palaeogeography at the Southeastern margin of the Kaapvaal-Grunehogna Craton. Gondwana Res. 6, 449–465. https://doi.org/10.1016/ S1342-937X(05)70998-9.
- Bingen, B., Jacobs, J., Viola, G., Henderson, I.H.C., Skår, B., R., Thomas, R.J., Solli, A., Key, R.M., Daudi, E.X.F., 2009. Geochronology of the Precambrian crust in the Mozambique belt in NE Mozambique, and implications for Gondwana assembly. Precambr. Res. 170, 231–255. https://doi.org/10.1016/j.precamres.2009.01.005.
- Bisnath, A., Frimmel, H.E., Armstrong, R.A., Board, W.S., 2006. Tectono-thermal evolution of the Maud Belt: New SHRIMP U-Pb zircon data from Gjelsvikfjella, Dronning Maud Land, East Antarctica. Precambr. Res. 150, 95–121. https://doi.org/10.1016/j.precamres.2006.06.009.
- Borrello, A.V., 1963. Sobre la geologia de las Islas Malvinas. Ministerio de Educación y Justica, Buenos Aires.
- Bouvier, A., Vervoort, J.D., Patchett, P.J., 2008. The Lu-Hf and Sm-Nd isotopic composition of CHUR: constraints from unequilibrated chondrites and implications for the bulk composition of terrestrial planets. Earth Planet. Sci. Lett. 273, 48–57.
- Bradshaw, J.D., Vaughan, A.P.M., Millar, I.L., Flowerdew, M.J., Trouw, R.A.J., Fanning, C.M., Whitehouse, M.J., 2012. Permo-Carboniferous conglomerates in the Trinity Peninsula Group at View Point, Antarctic Peninsula: sedimentology, geochronology and isotope evidence for provenance and tectonic setting in Gondwana. Geol. Mag. 149, 626-644. https://doi.org/10.1017/S001675681100080X.
- Bush, M.A., Saylor, J.E., Horton, B.K., Nie, J., 2016. Growth of the Qaidam Basin during Cenozoic exhumation in the northern Tibetan Plateau: Inferences from depositional patterns and multiproxy detrital provenance signatures. Lithosphere 8, 58–82. https://doi.org/10.1130/L449.1.
- Capaldi, T.N., McKenzie, N.R., Horton, B.K., Mackaman-Lofland, C., Colleps, C.L., Stockli, D.F., 2021. Detrital zircon record of Phanerozoic magmatism in the southern Central Andes. Geosphere 17, 1–22. https://doi.org/10.1130/ CFS0.2346 1
- Castillo, P., Lacassie, J., Augustsson, C., Hervé, F., 2015. Petrography and geochemistry of the Carboniferous-Triassic Trinity Peninsula Group, West Antarctica: Implications for provenance and tectonic setting. Geol. Mag. 152 (4), 575-588. https://doi.org/10.1017/S00167568140004541.
- Castillo, P., Fanning, C.M., Hervé, F., Lacassie, J.P., 2016. Characterization and tracing of Permian magmatism in the south-western segment of the Gondwanan margin; U-Pb age, Lu-Hf and O isotopic compositions of detrital zircons from metasedimentary complexes of northern Antarctic Peninsula and western Patagonia. Gondwana Res. 36, 1-13. https://doi.org/10.1016/j.gr.2015.07.014.
- Castillo, P., Fanning, C.M., Fernandez, R., Poblete, F., Hervé, F., 2017. Provenance and age constraints of Paleozoic siliciclastic rocks from the Ellsworth Mountains in West Antarctica, as determined by detrital zircon geochronology. Geol. Soc. Am. Bull. 129. 1568–1584. https://doi.org/10.1130/B31686.1.
- Cawood, P.A., 2005. Terra Australis orogen: Rodinia breakup and development of the Pacific and Iapetus margins of Gondwana during the Neoproterozoic and Paleozoic. Earth Sci. Rev. 69, 249–279. https://doi.org/10.1016/j.earscirev.2004.09.001.
- Cawood, P.A., Buchan, C., 2007. Linking accretionary orogenesis with supercontinent assembly. Earth Sci. Rev. 82, 217–256.
 Cecil, R., Gehrels, G., Patchett, J., Ducea, M., 2011. U-Pb-Hf characterization of the
- Cecil, R., Gehrels, G., Patchett, J., Ducea, M., 2011. U-Pb-Hf characterization of the central Coast Mountains batholith: implications for petrogenesis and crustal architecture. Lithosphere 3, 247–260.
- Chernicoff, C.J., Zappettini, E.O., Santos, J.O.S., McNaughton, N.J., Belousova, E., 2013. Combined U-Pb SHRIMP and Hf isotope study of the Late Paleozoic Yaminué Complex, Rio Negro Province, Argentina: Implications for the origin and evolution of the Patagonia composite terrane. Geosci. Front. 4, 37–56. https:// doi.org/10.1016/j.gsf.2012.06.003.
- Cingolani, C. A. and Varela, R., 1976. Investigaciones geológicas y geochronológicas en el extremo sur de la isla Gran Malvina, sector do Cabo Belgrano (Cabo Meredith), Islas Malvinas. In: Actas del 6° Congreso Geológico Argentino, Buenos Aires 1, 457-473.
- Condie, K.C., 2005. Earth as an Evolving Planetary System. Elsevier Academic Press, p. 447 pp..
- Cooper, M.R., Oosthuizen, R., 1974. Archaeocyatha-bearing erratics from the Dwyka Subgroup (Permo-Carboniferous) and their importance to continental drift. Nature 247. 396–398.
- Craddock, J.P., Fitzgerald, P., Konstantinou, A., Nereson, A., Thomas, R.J., 2017. Detrital zircon provenance of upper Cambrian-Permian strata and tectonic evolution of the Ellsworth Mountains. West Antarctica. Gondwana Res. 45, 191–207. https://doi.org/10.1016/j.gr.2016.11.011.
- Craddock, J.P., Ojakangas, R.W., Malone, D.H., Konstantinou, A., Mory, A., Bauer, W., Thomas, J., Affinati, S.C., Pauls, K., Botha, G., Rochas-Campos, A., Tohver, E., Riccomini, C., Martin, J., Redfern, J., Gehrels, G., 2019. Detrital zircon provenance of Permo-Carboniferous glacial diamictites across Gondwana. Earth Sci. Rev. 192, 285–316. https://doi.org/10.1016/j.earscirev.2019.01.014.

- Curtis, M.L., 2001. Tectonic history of the Ellsworth Mountains, West Antarctica: reconciling an Antarctic enigma. Geol. Soc. Am. Bull. 113, 939–958.
- Curtis, M.L., and Storey, B.C., 1996. A review of geological constraints on the prebreak-up position of the Ellsworth Mountains within Gondwana: implications for Weddell Sea evolution. In: Storey, B.C., King, E.C., Livermore, R.A. (Eds.), Weddell Sea Tectonics and Gondwana Break-up. J. Geol. Soc. London, Spec. Publ. 108. 11–30.
- Curtis, M.L., Hyam, D.M., 1998. Late Paleozoic to Mesozoic structural evolution of the Falkland Islands: a displaced segment of the Cape Fold Belt. J. Geol. Soc. London 155, 115–129.
- Curtis, M.L., Lomas, S.A., 1999. Late Cambrian stratigraphy of the Heritage Range, Ellsworth Mountains: implications for basin evolution. Antarctic Sci. 11, 63–77. https://doi.org/10.1017/S0954102099000103.
- Dahlquist, J.A., Pankhurst, R.J., Gaschnig, R.M., Rapela, C.W., Casquet, C., Alasino, P. H., Galindo, C., Baldo, E.G., 2013. Hf and Nd isotopes in Early Ordovician to early Carboniferous granites as monitors of crustal growth in the proto-Andean margin of Gondwana. Gondwana Res. 23, 1617–1630. https://doi.org/10.1016/j.gr.2012.08.013.
- Dahlquist, J.A., Alasino, P.H., Basei, M.A.S., Morales Cámera, M.M., Macchioli Grande, M., da Costa Campos Neto, M., 2018. Petrological, geochemical, isotopic, and geochronological constraints for the Late Devonian-early Carboniferous magmatism in SW Gondwana (27–32°LS): An example of geodynamic switching. Int. J. Earth Sci. 107, 2575–2603. https://doi.org/10.1007/s00531 018-1615-9.
- Dalziel, I.W.D., 2007. The Ellsworth Mountains: Critical and enduringly enigmatic, U.S. Geological Survey and The National Academies; USGS OF-2007-1047, Short Research Paper 004. In: 10th International Symposium on Antarctic Earth Sciences, https://doi.org/10.3133/of2007-1047.srp004. 5 pgs.
- Dalziel, I.W.D., Elliot, D.H., 1982. West Antarctica: Problem child of Gondwanaland. Tectonics 1, 3–19.
- Dalziel, I.W.D., Garrett, S.W., Grunow, A.M., Pankhurst, R.J., Storey, B.C., Vennum, W.
 R., 1987. The Ellsworth-Whitmore crustal block: its role in the tectonic evolution of West Antarctica: Gondwana Six: Structure Tectonics and Geophysics. Am Geophys Union Geophys Monogr 40, 173–182.
- Dalziel, I.W.D., Grunow, A.M., 1992. Late Gondwanide Tectonic Rotations within Gondwanaland. Tectonics 11, 603–606.
- Dalziel, I.W.D., Lawver, L.A., Murphy, B., 2000. Plumes, orogenesis, and supercontinental fragmention: Earth Planet. Sci. Lett. 178 (1–2), 1–11.
- Dalziel, I.W.D., Lawver, L.A., Norton, I.O., Gahagan, L.M., 2013. The Scotia Arc: Genesis, Evolution, Global Significance. Annu. Rev. Earth Planet. Sci. 41, 767–793
- Darwin, C. R., 1846. On the geology of the Falkland Islands: Quarterly J. Geol. Soc. London 2, 267-27.
- De Waele, B., Wingate, M.T.D., Fitzsimons, I.C.W., Mapani, B.S.E., 2003. Untying the Kibaran knot: a reassessment of Mesoproterozoic correlations in southern Africa based on SHRIMP U-Pb data from the Irumide belt. Geology 31, 509–512. https://doi.org/10.1130/0091-7613(2003)031<0509:UTKKAR>2.0. CO:2.
- De Waele, B., Kampunzu, A.B., Mapani, B.S.E., Tembo, F., 2006. The Mesoproterozoic Irumide belt of Zambia. J. Afr. Earth Sci. 46, 36–70. https://doi.org/10.1016/j.jafrearsci.2006.01.018.
- del Rey, A., Deckart, K., Arriagada, C., Martínez, F., 2016. Resolving the paradigm of the late Paleozoic-Triassic Chilean magmatism. Isotopic approach: Gondwana Res. 37, 172–181. https://doi.org/10.1016/j.gr.2016.06.008.
- Dickinson, W.R., Suczek, C.A., 1979. Plate tectonics and sandstone compositions. AAPG Bull. 63, 2164–2182.
- Dickinson, W.R., Beard, L.S., Brakenridge, G.R., Erjavec, J.L., Ferguson, R.C., Inman, K. F., Knepp, R.A., Lindberg, F.A., Ryberg, P.T., 1983. Provenance of North American Phanerozoic sandstones in relation to tectonic setting. Geol. Soc. Am. Bull. 94, 222. https://doi.org/10.1130/0016-7606(1983)94<222:PONAPS>2.0.CO;2.
- Du Toit, A.L., 1927. A geological comparison of South America with South Africa. Carnegie Institution, Washington, p. 158.
- Du Toit, A.L., 1937. Our Wandering Continents. Oliver and Boyd, Edinburgh and London, p. 366.
- Ducea, M.N., Otamendi, J.E., Bergantz, G., Stair, K.M., Valencia, V.A., and Gehrels, G., 2010. Timing constraints on building an intermediate plutonic arc crustal section. U-Pb zircon geochronology of the Sierra Valle Fertil-La Huerta, Famatinian arc, Argentina. Tectonics 29, 1-22, https://doi.org/10.1029/2009TC002615
- Eagles, G., Eisermann, H., 2020. The Skytrain plate and tectonic evolution of southwest Gondwana since Jurassic times. Sci. Rep. 10, 1–17. https://doi.org/ 10.1038/s41598-020-77070-6.
- Elliot, D.H., Fanning, C.M., Laudon, T.S., 2016. The Gondwana Plate margin in the Weddell Sea sector: Zircon geochronology of Upper Paleozoic (mainly Permian) strata from the Ellsworth Mountains and eastern Ellsworth Land. Antarctica. Gondwana Res. 29, 234–247. https://doi.org/10.1016/j.gr.2014.12.001.
- Elliot, D.H., 2013. The geological and tectonic evolution of the Transantarctic Mountains: a review. In: Hambrey, M.J., Barker, P.F., Barrett, P.J., Bowman, V., Davies, B., Smellie, J.L., Tranter, M. (Eds.), Antarctic Palaeoenvironments and Earth-Surface Processes. J. Geol. Soc. London, Spec. Publ. 381, 7–35. http:// dx.doi.org/ 10.1144/SP381.14.
- Flowerdew, M.J., Millar, I.L., Curtis, M.L., Vaughan, A.P.M., Horstwood, M.S.A., Whitehouse, M.J., Fanning, C.M., 2007. Combined U-Pb geochronology and Hf isotope geochemistry of detrital zircons from early Paleozoic sedimentary rocks, Ellsworth-Whitmore Mountains block. Antarctica. Geol. Soc. Am. Bull. 119, 275–288. https://doi.org/10.1130/B25891.1.

- Fourie, P.H., Zimmermann, U., Beukes, N.J., Naidoo, T., Kobayashi, K., Kosler, J., Nakamura, E., Tait, J., Theron, J.N., 2011. Provenance and reconnaissance study of detrital zircons of the Paleozoic Cape Supergroup in South Africa. revealing the interaction of the Kalahari and Río de la Plata cratons. Int. J. Earth Sci. 100, 527–541. https://doi.org/10.1007/s00531-010-0619-x.
- Frakes, L.A., Crowell, J.C., 1967. Facies and paleogeography of Late Paleozoic Diamictite, Falkland Islands. Geol. Soc. Am. Bull. 78, 37–58.
- Frimmel, H.E., Basei, M.A.S., Correa, V.X., Mbangula, N., 2013. A new lithostratigraphic subdivision and geodynamic model for the Pan-African western Saldania Belt, South Africa. Precambr. Res. 231, 218–235. https://doi.org/10.1016/j. precamres.2013.03.014.
- Garzanti, E., 2019. Petrographic classification of sand and sandstone. Earth Sci. Rev. 192, 545–563. https://doi.org/10.1016/j.earscirev.2018.12.014.
- Garzanti, E., Doglioni, C., Vezzoli, G., Andò, S., 2007. Orogenic Belts and Orogenic Sediment Provenance. J. Geol. 115, 315–334. https://doi.org/10.1086/512755.
- Gaucher, C., Boggiani, P.C., Sprechmann, P., Sial, A.N., Fairchild, T., 2003. Integrated correlation of the Vendian to Cambrian Arroyo del Soldado and Corumb´a groups (Uruguay and Brazil): Palaeogeographic, palaeoclimatic and palaeobiologic implications. Precambr. Res. 120, 241–278. https://doi.org/10.1016/S0301-9268 (02)00140-7.
- Gehrels, G., Pecha, M., 2014. Detrital zircon U-Pb geochronology and Hf isotope geochemistry of Paleozoic and Triassic passive margin strata of western North America. Geosphere 10, 49–65. https://doi.org/10.1130/GES00889.1.
- . Detrital zircon geochronology by laser-ablation multicollector ICPMS at the Arizona LaserChron center 11, 1–10.
- Gehrels, G.E., Valencia, V., Ruiz, J., 2008. Enhanced precision, accuracy, efficiency, and spatial resolution of U-Pb ages by laser ablation—multicollector—inductively coupled plasma— mass spectrometry. Geochem. Geophy. Geosystems. 9, 1–13. https://doi.org/10.1029/2007GC001805.
- Gianni, G.M., Navarrete, C.R., 2022. Catastrophic slab loss in southwestern Pangea preserved in the mantle and igneous record. Nature Comm. 13, 698. https://doi. org/10.1038/s41467-022-28290-z.
- González, P.D., Tortello, M.F., Damborenea, S.E., Naipauer, M., Sato, A.M., Varela, R., 2013. Archaeocyaths from South America: review and a new record. Geol. J. 48, 114, 125
- Goodge, J.W., Fanning, C.M., Bennett, V.C., 2001. U-Pb evidence of ∼1.7 Ga crustal tectonism during the Nimrod Orogeny in the Transantarctic Mountains, Antarctica: implications for Proterozoic plate reconstructions. Precambr. Res. 112, 261–288. https://doi.org/10.1016/S0301-9268(01)00193-0.
- Goodge, J.W., Fanning, C.M., 2016. Mesoarchean and Paleoproterozoic history of the Nimrod Complex, central Transantarctic Mountains, Antarctica: Stratigraphic revisions and relation to the Mawson Continent in East Gondwana. Precambr. Res. 285, 242–271. https://doi.org/10.1016/j.precamres.2016.09.001.
- Goscombe, B., Foster, D.A., Gray, D., Wade, B., 2020. Assembly of central Gondwana along the Zambezi Belt: metamorphic response and basement reactivation during the Kuunga Orogeny. Gondwana Res. 80, 410–465.
- Gregori, D., Strazzere, L., Barros, M., Benedini, L., Marcos, P., Kostadinoff, J., 2020. The Mencué Batholith: Permian episodic arc-related magmatism in the western North Patagonian Massif. Argentina. Int. Geol. Rev. 63, 1–25.
- Gresse, P.G., Theron, J.N., Fitch, F.J., Miller, J.A., 1992. Tectonic inversion and radiometric resetting of the basement of the Cape Fold belt. In: de Wit, M.J., Ransome, I.G.D. (Eds.), Inversion Tectonics of the Cape Fold Belt, Karoo and Cretaceous Basins of Southern Africa. Balkema, Rotterdam, pp. 217–228.
- Griffis, N.P., Montañez, I.P., Fedorchuk, N., Isbell, J., Mundil, R., Vesely, F., Weinshultz, L., Iannuzzi, R., Gulbranson, E., Taboada, A., Pagani, A., Sanborn, M.E., Huyskens, M., Wimpenny, J., Linol, B., Yin, Q.Z., 2019. Isotopes to ice: Constraining provenance of glacial deposits and ice centers in west-central Gondwana. Palaeogeogr. Palaeocl. Palaeoec. 531, 108745. https://doi.org/10.1016/j.ipalaeo.2018.04.020
- Grunow, A.M., Kent, D.V., Dalziel, I.W.D., 1987. Mesozoic evolution of West Antarctica and the Weddell Sea Basin: new paleomagnetic constraints. Earth Planet. Sci. Lett. 86, 16–26.
- Guynn, J., Gehrels, G.E., 2010. Comparison of detrital zircon age distributions in the K-S test: Tucson. University of Arizona, Arizona LaserChron Center, pp. 1–16.
- Hälbich, I.W., Fitch, F.J., Miller, J.A., 1983, Dating the Cape Orogeny. In: Söhnge, A.P. G., Hälbich, I.W. (Eds.), Geodynamics of the Cape Fold Belt. Geol. Soc. South Afr., Spec. Publ. 12, 149–164.
- Hartmann, L.A., Santos, J.O.S., Bossi, J., Campal, N., Schipilov, A., McNaughton, N.J., 2002. Zircon and titanite U-Pb SHRIMP geochronology of Neoproterozoic felsic magmatism on the eastern border of the Rio de la Plata Craton. Uruguay. J. South Am. Earth Sci. 15, 229–236. https://doi.org/10.1016/S0895-9811(02) 00030-5.
- Hiller, N., Taylor, F.F., 1992. Late Devonian shoreline changes: an analysis of Witteberg Group stratigraphy in the Grahamstown area. S. Afr. J. Geol. 95, 203–212
- Hole, M.J., Ellam, R.M., MacDonald, D.I.M., Kelley, S.P., 2016. Gondwana break-up related magmatism in the Falkland Islands. J. Geol. Soc, London 173, 108–126. https://doi.org/10.1144/jgs2015-027.
- Horton, B.K., Constenius, K.N., DeCelles, P.G., 2004. Tectonic control on coarse-grained foreland-basin sequences: An example from the Cordilleran foreland basin. Utah Geol. 32, 637. https://doi.org/10.1130/G20407.1.
- Hunter, M.A., Lomas, S.A., 2003. Reconstructing the Siluro-Devonian coastline of Gondwana: insights from the sedimentology of the Port Stephens Formation, Falkland Islands. J. Geol. Soc, London 160, 459–476.

- Ingersoll, R.V., Bullard, T.F., Ford, R.L., Grimm, J.P., Pickle, J.D., Sares, S.W., 1984. The effect of grain size on detrital modes: a test of the Gazzi-Dickinson point-counting method. J. Sed. Petrology 54, 103–116.
- Isbell, J.L., Cole, D.I., Catuneanu, O., 2008. Carboniferous-Permian glaciation in the main Karoo Basin, South Africa: stratigraphy, depositional controls, and glacial dynamics. Geol. Soc. Am. Spec. Pap. 441, 71–82.
- Isbell, J.L., Henry, L.C., Gulbranson, E.L., Limarino, C.O., Fraiser, M.L., Koch, Z.J., Ciccioli, P.L., Dineen, A.A., 2012. Glacial paradoxes during the late Paleozoic ice age: Evaluating the equilibrium line altitude as a control on glaciation. Gondwana Res. 22, 1–19. https://doi.org/10.1016/j.gr.2011.11.005.
- Jacobs, J., Fanning, C.M., Henjes-Kunst, F., Olesch, M., Paech, H.J., 1998. Continuation of the Mozambique Belt into East Antarctica: Grenville-age metamorphism and polyphase Pan-African high-grade events in central Dronning Maud Land. J. Geol. 106, 385–406. https://doi.org/10.1086/516031.
- Jacobs, J., Thomas, R.J., Armstrong, R.A., Henjes-Kunst, F., 1999. Age and thermal evolution of the Mesoproterozoic Cape Meredith Complex, West Falkland. J. Geol. Soc. London 156, 917–928.
- Jacobs, J., Bauer, W., Fanning, C.M., 2003. Late Neoproterozoic/early Paleozoic events in central Dronning Maud Land and significance for the southern extension of the East African Orogen into East Antarctica. Precambr. Res. 126, 27–53 10. 1016/S0301-9268(03)00125-6.
- Jordan, T.A., Ferraccioli, F., Leat, P.T., 2016. New geophysical compilations link crustal block motion to Jurassic extension and strike-slip faulting in the Weddell Sea Rift System of West Antarctica. Gondwana Res. 42, 29–48. https:// doi.org/10.1016/j.gr.2016.09.009.
- Kay, S.M., Ramos, V.A., Mpodozis, C., Sruoga, P., 1989. Late Paleozoic to Jurassic silicic magmatism at the Gondwana margin: analogy to the Middle Proterozoic in North America? Geology 17, 324–328.
- Kleiman, L.E., Japas, M.S., 2009. The Choiyoi volcanic province at 34°S-36°S (San Rafael, Mendoza, Argentina): Implications for the late Paleozoic evolution of the south-western margin of Gondwana. Tectonophysics 473 (3-4), 283-299. https://doi.org/10.1016/j.tecto.2009.02.046.
- Kristoffersen, M., Andersen, T., Elburg, M.A., Watkeys, M.K., 2016. Detrital zircon in a supercontinental setting: locally derived and far-transported components in the Ordovician Natal Group, South Africa. J. Geol. Soc. 173, 203–215 10.1144/ ips2015-012.
- Kröner, A., 2001. The Mozambique belt of East Africa and Madagascar: significance of zircon and Nd model ages for Rodinia and Gondwana supercontinent formation and dispersal. South Afr. J. Geol. 104, 151–166. https://doi.org/ 10.2113/1040151.
- Kröner, A., Stern, R.J., 2004. Pan African orogeny. Encyclopedia of Geology 1, 1–12. https://doi.org/10.1016/B0-12369396-9/00431-7.
- Kröner, A., Willner, A.P., Hegner, E., Jaeckel, P., Nemchin, A., 2001. Single zircon ages, PT evolution and Nd isotopic systematics of high-grade gneisses in southern Malawi and their bearing on the evolution of the Mozambique belt in southeastern Africa. Precambr. Res. 10, 257–291. https://doi.org/10.1016/S0301-9268(01)00150-4.
- Lawrence, S.R., Johnson, M., Tubb, S.R., and Marshall, S.J., 1999. Tectonostratigraphic evolution of the North Falkland region. In: Cameron, N.R., Bate, R.H. and Clure, V.S. (eds) The Oil and Gas Habitats of the South Atlantic. J. Geol. Soc. London, Spec. Publ. 153, 409–424, https://doi. org/10.1144/GSL.SP.1999.153.01.25.
- Li, Z.X., Bogdanova, S.V., Collins, A.S., Davidson, A., De Waele, B., Ernst, I.C.W., Fitzsimons, R.E., Fuck, R.A., Gladkochub, D.P., Jacobs, J., Karlstrom, K.E., Lu, S., Natapov, L.M., Pease, V., Pisarevsky, S.A., Thrane, K., Vernikovsky, V., 2008. Assembly, configuration, and break-up history of Rodinia: a synthesis. Precambr. Res. 160, 179–210. https://doi.org/10.1016/j.precamres.2007.04.021.
- López-Gamundí, O.R., 1997. Glacial-postglacial transition in the late Paleozoic basins of Southern South America. In: Martini, I.P. (Ed.), Late Glacial and Postglacial Environmental Changes: Quaternary Carboniferous-Permian, and Proterozoic. Oxford University Press, Oxford U.K., pp. 147–168.
 López-Gamundí, O., Limarino, C.O., Isbell, J.L., Pauls, K., Césari, S.N., Alonso-Muruaga,
- López-Gamundí, O., Limarino, C.O., Isbell, J.L., Pauls, K., Césari, S.N., Alonso-Muruaga, P.J., 2021. The late Paleozoic Ice Age along the southwestern margin of Gondwana: Facies models, age constraints, correlation and sequence stratigraphic framework. J. South Am. Earth Sci. 107, 103056. https://doi.org/10.1016/j.jsames.2020.103056.
- Lovecchio, J.P., Naipauer, M., Cayo, L.E., Rohais, S., Giunta, D., Flores, G., Gerster, R., Bolatti, N.D., Joseph, P., Valencia, V.A., Ramos, V.A., 2019. Rifting evolution of the Malvinas basin, offshore Argentina: New constrains from zircon U-Pb geochronology and seismic characterization. J. South Am. Earth Sci. 95, 102253. https://doi.org/10.1016/j.jsames.2019.102253.
- Macdonald, D., Gomez-Perez, I., Franzese, J., Spalletti, L., Lawver, L., Gahagan, L., Dalziel, I., Thomas, C., Trewin, N., Hole, M., Paton, D., 2003. Mesozoic break-up of SW Gondwana: implications for regional hydrocarbon potential of the southern South Atlantic. Mar. Petrol. Geol. 20, 287–308. https://doi.org/10.1016/S0264-8172(03)00045-X.
- Marshall, J.E.A., 1994. The Falkland Islands: A key element in Gondwana paleogeography. Tectonics 13, 499–514. https://doi.org/10.1029/93TC03468.
- Marshall, J.E.A., 2016. Palynological calibration of Devonian events at near-polar palaeolatitudes in the Falkland Islands, South America. In: Becker, R. T., Königshof, P. & Brett, C. (eds) Devonian Climate, Sea Level and Evolutionary Events. Geol. Soc. London, Spec. Publ. 423, 25–44.
- Martin, E.L., Collins, W.J., and Spencer, C.J., 2019. Laurentian origin of the Cuyania suspect terrane, western Argentina, confirmed by Hf isotopes in zircon. Geol. Soc. Am. Bull. 132, 273–290, https://doi.org/10.1130 /B35150.1.

- Meadows, N.S., 1999. Basin evolution and sedimentary fill in the Paleozoic sequences of the Falkland Islands. In Cameron, N. R., Bate, R. H. and Clure, V. S. (eds) The Oil and Gas Habitats of the South Atlantic. Geol. Soc. London, Spec. Publ. 153, 445–464.
- Mitchell, C., Taylor, G.K., Cox, K.G., Shaw, J., 1986. Are the Falkland Islands a rotated microplate? Nature 319, 131–134. https://doi.org/10.1038/319131a0.
- Mitchell, C., Ellam, R.M., Cox, K.G., 1999. Mesozoic dolerite dykes of the Falkland Islands: petrology, petrogenesis and implications for geochemical provinciality in Gondwanaland low-Ti basaltic rocks. J. Geol. Soc. London 156, 901–916.
- Montañez, I.P., McElwain, J.C., Poulsen, C.J., White, J.D., DiMichele, W.A., Wilson, J.P., Griggs, G., Hren, M.T., 2016. Climate, pCO2 and terrestrial carbon cycle linkages during late Palaeozoic glacial-interglacial cycles. Nature Geosci. 9, 824–828. https://doi.org/10.1038/ngeo2822.
- Morris, J., Sharpe, D., 1846. Description of eight species of brachiopodous shells from the Paleozoic rocks of the Falkland Islands. Quarterly J. Geol. Soc. London 2, 274–278.
- Morton, A.C., Hallsworth, C., 1994. Identifying provenance-specific features of detrital heavy mineral assemblages in sandstones. Sed. Geol. 90, 241–256. https://doi.org/10.1016/0037-0738(94)90041-8.
- Morton, A.C., Hallsworth, C.R., 1999. Processes controlling the composition of heavy mineral assemblages in sandstones. Sed. Geol. 124, 3–29. https://doi.org/ 10.1016/S0037-0738(98)00118-3.
- Mussett, A.E., Taylor, G.K., 1994. 40Ar-39Ar ages for dykes from the Falkland Islands with implications for the break-up of southern Gondwanaland. J. Geol. Soc. London 151, 79-81. https://doi.org/10.1144/gsjgs. 151.1.0079.
- Nelson, D.A., Cottle, J.M., 2019. Tracking voluminous Permian volcanism of the Choiyoi Province into central Antarctica. Lithosphere 11, 386–398. https://doi. org/10.1130/L1015.1.
- Nie, J., Horton, B.K., Saylor, J.E., Mora, A., Mange, M., Garzione, C.N., Basu, A., Moreno, C.J., Caballero, V., Parra, M., 2012. Integrated provenance analysis of a convergent retroarc foreland system: U-Pb ages, heavy minerals, Nd isotopes, and sandstone compositions of the Middle Magdalena Valley basin, northern Andes. Colombia. Earth Sci. Rev. 110, 111–126. https://doi.org/10.1016/j.earscirey.2011.11.002.
- Nxumalo, V., 2012. Uranium Mineralization and Provenance Analyses of the Karoo Supergroup in the Springbok Flats Coalfield, South Africa. University of Johannesburg, Johannesburg, Doctoral Thesis):.
- Oliveros, V., Vásquez, P., Creixell, C., Lucassen, F., Ducea, M.N., Ciocca, I., González, J., Espinoza, M., Salazar, E., Coloma, F., Kasemann, S., 2020. Lithospheric evolution of the Pre-and Early Andean convergent margin. Chile. Gondwana Res. 80, 202–227. https://doi.org/10.1016/j.gr.2019.11.002.
- Oyhantçabal, P., Siegesmund, S., Wemmer, K., Presnyakov, S., Layer, P., 2009. Geochronological constraints on the evolution of the southern Dom Feliciano Belt (Uruguay). J. Geol. Soc. London 166, 1075–1084.
- Pankhurst, R.J., Rapela, C.W., Fanning, C.M., Márquez, M., 2006. Gondwanide continental collision and the origin of Patagonia. Earth Sci. Rev. 76, 235–257.
- Perejón, A., Rodríguez-Martínez, M., Moreno-Eiris, E., Menéndez, S., Reitner, J., 2019. First microbial-archaeocyathan boundstone record from early Cambrian erratic cobbles in glacial diamictite deposits of Namibia (Dwyka Group, Carboniferous). J. Syst. Palaeontol. 17, 881–910.
- Pettijohn, F.J., 1975. Sedimentary rocks. Harper and Row New York.
- Ramos, V.A., and Folguera, A., 2009. Andean flat-slab subduction through time, in Murphy, J.B., et al., eds., Ancient Orogens and Modern Analogues. Geol. Soc. London, Spec. Publ. 327, 31–54, https://doi.org/10.1144/SP327.3.
- Ramos, V.A., Naipauer, M., 2014. Patagonia: where does it come from? J. Iber. Geol. 40 (2), 367–379.
- Ramos, V.A., Jordan, T.E., Allmendinger, R.W., Kay, S.M., Cortés, J.M., Palma, M., 1984. Chilenia: Un terreno alóctono en la evolución paleozoica de los Andes centrales: Congreso Geológico Argentino, 9th. Bariloche, Argentina, Abstracts 2, 84–106.
- Ramos, V.A., Chemale, F., Naipauer, M., Pazos, P.J., 2014. A provenance study of the Paleozoic Ventania System (Argentina): Transient complex sources from Western and Eastern Gondwana. Gondwana Res. 26, 719–740. https://doi.org/10.1016/j.gr.2013.07.008.
- Ramos, V.A., Cingolani, C., Chemale, F., Naipauer, M., Rapalini, A., 2017. The Malvinas (Falkland) Islands revisited: The tectonic evolution of southern Gondwana based on U-Pb and Lu-Hf detrital zircon isotopes in the Paleozoic cover. J. South Am. Earth Sci. 76, 320–345.
- Ramos, V.A., Chemale, F., Lovecchio, J.P., Naipauer, M., 2019. The Malvinas (Falkland)
 Plateau derived from Africa? Constraints for its tectonic evolution. Science
 reviews from the end of the world 1, 6–18.
- Randall, D.E., MacNiocaill, C., 2004. Cambrian paleomagnetic data confirm a Natal Embayment location for the Ellsworth-Whitmore Mountains. Int. Geophys. J. 157, 105–116.
- Rapalini, A.E., 2018. The assembly of western Gondwana: Reconstruction based on paleomagnetic data, in Siegesmund, S., ed., Geology of Southwest Gondwana. Cham, Switzerland, Springer, 3–18, https://doi.org/10.1007/978 -3-319-68920-3 1.
- Rapela, C.W., Pankhurst, R.J., Casquet, C., Fanning, C.M., Baldo, E.G., González Casado, J.M., Galindo, C., Dahlquist, J., 2007. The Río de la Plata craton and the assembly of SW Gondwana. Earth Sci. Rev. 83, 49–82. https://doi.org/10.1016/j.earscirev.2007.03.004.
- Rapela, C.W., Verdecchia, S.O., Casquet, C., Pankhurst, R.J., Baldo, E.G., Galindo, C., Murra, J.A., Dahlquist, J.A., Fanning, C.M., 2016. Identifying Laurentian and SW Gondwana sources in the Neoproterozoic to early Paleozoic metasedimentary rocks of the Sierras Pampeanas. Paleogeographic and tectonic implications. Gondwana Res. 32, 193–212. https://doi.org/10.1016/j.gr.2015.02.010.

- Richards, P.C., Gatliff, R.W., Quinn, M.F., Williamson, J.P., and Fannin, N.G.T., 1996. The geological evolution of the Falkland Islands continental shelf. In: Storey, B. C., King, E. C. and Livermore, R. A. (eds) Weddell Sea Tectonics and Gondwana Break-up. Geol. Soc. London, Spec. Publ. 108, 105-128.
- Richards, P.C., Stone, P., Kimbell, G.S., McIntosh, W.C., Phillips, E.R., 2013. Mesozoic magmatism in the Falkland Islands (South Atlantic) and their offshore sedimentary basins. J. Petrol. Geol. 36, 61–74.
- Riley, T.R., Flowerdew, M.J., Whitehouse, M.J., 2012. U-Pb ion-microprobe zircon geochronology from the basement inliers of eastern Graham land. Antarctic Peninsula. J. Geol. Soc. London 169, 381–393.
- Riley, T.R., Flowerdew, M.J., Pankhurst, R.J., Millar, I.L., Whitehouse, M.J., 2020. U-Pb zircon geochronology from Haag Nunataks, Coats Land and Shackleton Range (Antarctica): Constraining the extent of juvenile Late Mesoproterozoic arc terranes. Precambr. Res. 340, 105646. https://doi.org/10.1016/j.precamres.2020.105646.
- Rodríguez-Martínez, M., Buggisch, W., Menéndez, S., Moreno-Eiris, E., Perejón, A., 2022. Reconstruction of a lost Cambrian Series 2 mixed siliciclastic–carbonate platform from carbonate clasts of the Shackleton Range, Antarctica. Earth Environ. Sci. Trans. R. Soc. Edinb. 113, 175–226.
- Rosa, E.L.M., Isbell, J.L., 2021. Late Paleozoic Glaciation. Encyclopedia of Geology. Elsevier, 534–545.
- Saylor, J.E., and K.E. Sundell, 2016. Quantifying comparison of large detrital geochronology data sets. Geosphere 12(1), 1–18, doi:10.1130/ GES01237.1.
- Saylor, J.E., Jordan, J.C., Sundell, K.E., Wang, X., Wang, S., Deng, T., 2018. Topographic growth of the Jishi Shan and its impact on basin and hydrology evolution. NE Tibetan Plateau. Basin Res. 30, 544–563. https://doi.org/10.1111/bre.12264.
- Scasso, R., Mendía, J., 1985. Rasgos estratigraficos y paleoambientales del Paleozoico de las Islas Malvinas. Rev. Association Geology Argentina 40 (1–2), 26–50
- Schwartz, J.J., Gromet, L.P., Miro, R., 2008. Timing and duration of the calc-alkaline arc of the Pampean orogeny: Implications for the late Neoproterozoic to Cambrian evolution of western Gondwana. J. Geol. 116, 39–61. https://doi.org/ 10.1086/524122.
- Sharman, G.R., Sharman, J.P., Sylvester, Z., 2018. detritalPy: A Python-based toolset for visualizing and analysing detrital geo-thermochronologic data. The Depositional Record 4, 202–215. https://doi.org/10.1002/dep2.45.
- Simões, M.G., Quaglio, F., Warren, L.V., Anelli, L.E., Stone, P., Riccomini, C., Grohmann, C.H., Chamani, M.A.C., 2012. Permian non-marine bivalves of the Falkland Islands and their palaeoenvironmental significance. Alcheringa 36, 543-554.
- Sims, J.P., Ireland, T.R., Camacho, A., Lyons, P., Pieters, P.E., Skirrow, R.G., Stuart-Smith, P.G., and Miró, R., 1998. U-Pb, Th-Pb and Ar-Ar geochronology from the southern Sierras Pampeanas, Argentina: Implications for the Palaeozoic tectonic evolution of the western Gondwana margin. Geol. Soc. London, Spec. Publ. 142, 259-281, https://doi.org/10.1144/GSL.SP.1998.142.01.13.
- Stanca, R.M., Paton, D.A., Hodgson, D.M., McCarthy, D.J., Mortimer, E.J., 2019. A revised position for the rotated Falkland Islands microplate. J. Geol. Soc. London 176, 417–429.
- Stanca, R.M., McCarthy, D.J., Paton, D.A., Hodgson, D.M., Mortimer, E.J., 2022. The tectono-stratigraphic architecture of the Falkland Plateau basin; implications for the evolution of the Falkland Islands Microplate. Gondwana Res. 105, 320–342. https://doi.org/10.1016/j.gr.2021.09.014.
- Stone, P., 2021. Ray Adie and his 1952 proposal that the Falkland Islands had rotated How has it fared? Falkland Islands J. 11 (5), 50–71.
- Stone, P., and Thomson, M.R.A., 2005. Archaeocyathan limestone blocks of likely Antarctic origin in Gondwanan tillite from the Falkland Islands. In Vaughan, A. P. M., Leat, P. T. and Pankhurst, R. J. (eds) Terrane Processes at the Margins of Gondwana. Geol. Soc. London, Spec. Publ. 246, 347–357. London and Bath: Geological Society Publishing House. 446 pp.
- Stone, P., Kimbell, G.S., Richards, P.C., 2009. Rotation of the Falklands microplate reassessed after recognition of discrete Jurassic and Cretaceous dyke swarms. Petroleum Geosci. 15, 279–287.
- Stone, P., Thomson, M.R.A., Rushton, A.W.A., 2012. An Early Cambrian archaeocyathtrilobite fauna in limestone erratics from the Upper Carboniferous Fitzroy Tillite Formation, Falkland Islands. Earth Environ. Sci. Trans. R. Soc. Edinb. 102, 201– 225.
- Stone, P., 2016. Geology reviewed for the Falkland Islands and their offshore sedimentary basins: Earth and Environmental Science Transactions of the Royal Society of Edinburgh 106, 115-143.
- Storey, B.C., Hole, M.J., Pankhurst, R.J., Millar, I.L., Vennum, W., 1988. Middle Jurassic within-plate granites in West Antarctica and their bearing on the break-up of Gondwanaland. J. Geol. Soc. London 145, 999–1007.
- Storey, B.C., Curtis, M.L., Ferris, J.K., Hunter, M.A., Livermore, R.A., 1999. Reconstruction and break-out model for the Falkland Islands within Gondwana. J. Afr. Earth Sci. 29, 153–163.
- Sundell, K.E., Gehrels, G.E., Pecha, M.E., 2021. Rapid U-Pb Geochronology by Laser Ablation Multi-Collector ICP-MS. Geostand. Geoanal. Res. 45, 37–57. https://doi.org/10.1111/ggr.12355.
- Sundell, K.E., Macdonald, F.A., 2022. The tectonic context of hafnium isotopes in zircon. Earth Planet. Sci. Lett. 584, 117426. https://doi.org/10.1016/j. epsl.2022.117426.
- Tankard, A., Welsink, H., Aukes, P., Newton, R., Stettler, E., 2009. Tectonic evolution of the Cape and Karoo basins of South Africa. Mar. Petrol. Geol. 26, 1379–1412. https://doi.org/10.1016/j.marpetgeo.2009.01.022.
- Taylor, G.K., and Shaw, J., 1989. The Falkland Islands: New palaeomagnetic data and their origin as a displaced terrane from southern Africa. In: Hillhouse, J. W. (ed.)

- Deep structure and past kinematics of accreted terranes (IUGG Volume 5). AGU Geophys. Mono. 50, 59-72.
- Thistlewood, L., Randall, D., 1998. Palaeomagnetic studies of West Gondwanan microplates. J. Afr. Earth Sci. 27, 227.
- Thomas, W.A., Astini, R.A., Mueller, P.A., McClelland, W., 2015. Detrital-zircon geochronology and provenance of the Ocloyic synorogenic clastic wedge, and Ordovician accretion of the Argentine Precordillera terrane. Geosphere 11, 1749–1769. https://doi.org/10.1130/GES01212.1.
- Thomson, K., 1998. When did the Falklands rotate? Mar. Petrol. Geol. 15, 723–736. https://doi.org/10.1016/S0264-8172(98)00050-6.
- Trewin, N.H., Macdonald, D.I.M., Thomas, C.G.C., 2002. Stratigraphy and sedimentology of the Permian of the Falkland Islands: lithostratigraphic and palaeoenvironmental links with South Africa. J. Geol. Soc. London 159, 5–19.
- Uriz, N.J., Cingolani, C.A., ChemaleJr., F., Macambira, M.B., Armstrong, R., 2011. Isotopic studies on detrital zircons of Silurian-Devonian siliciclastic sequences from Argentinean North Patagonia and Sierra de la Ventana regions: comparative provenance. Int. J. Earth Sci. (Geologische Rundschau) 100, 571– 589.
- Vermeesch, P., Resentini, A., Garzanti, E., 2016. An R package for statistical provenance analysis. Sed. Geol. 336, 14–25. https://doi.org/10.1016/j.sedgeo.2016.01.009.
- Vermeesch, P., 2012. On the visualization of detrital age distributions. Chem. Geol. 312, 190–194, https://doi.org/10.1016/j.chemgeo.2012.04.021.
- Vervoort, J.D., Blichert-Toft, J., 1999. Evolution of the depleted mantle: Hf isotope evidence from juvenile rocks through time. Geochim. Cosmochim. Acta 63, 533–556
- Vervoort, J.D., Patchett, P.J., 1996. Behavior of hafnium and neodymium isotopes in the crust: constraints from Precambrian crustally derived granites. Geochim. Cosmochim. Acta 60, 3717–3733.
- Viglietti, P.A., Frei, D., Rubidge, B.S., Smith, R.M.H., 2018. U-Pb detrital zircon dates and provenance data from the Beaufort Group (Karoo Supergroup) reflect sedimentary recycling and air-fall tuff deposition in the Permo-Triassic Karoo foreland basin. J. Afr. Earth Sci. 143, 59–66. https://doi.org/10.1016/ j.jafrearsci.2017.11.006.

- Visser, J.N.J., 1997a. A review of the Permo-Carboniferous glaciation in Africa. In:
 Martini, I.P. (Ed.), Late Glacial and Postglacial Environmental Changes:
 Quaternary, Carboniferous-Permian, and Proterozoic. Oxford University Press,
 Oxford, U.K., pp. 169–191.
- Visser, J.N.J., 1997b. Deglaciation sequences in the Permo-Carboniferous Karoo and Kalahari basins of southern Africa: a tool in the analysis of cyclic glaciomarine basin fills. Sedimentology 44, 507–521.
- Visser, J.N.J., van Niekerk, B.N., van der Merwe, S.W., 1997. Sediment transport of the late Palaeozoic glacial Dwyka Group in the southwestern Karoo Basin. South Afr. J. Geol. 100, 223–236.
- Vorster, C., Kramers, J., Beukes, N., Van Niekerk, H., 2016. Detrital zircon U-Pb ages of the Palaeozoic Natal Group and Msikaba Formation, Kwazulu-Natal, South Africa: Provenance areas in context of Gondwana. Geol. Mag. 153, 460–486, https://doi.org/10.1017/S0016756815000370.
- Vorster, C., Kramers, J.D., Beukes, N.J., and Penn-Clarke, C.R., 2021. Long-lived stable shelf deposition along Gondwana's southern margin during the Ordovician-Silurian: Inferences from U Pb detrital zircon ages of the Table Mountain Group (South Africa) and correlatives in Argentina and the Falklands/Malvinas Islands. Chem. Geol. 576, 1-28, doi https://doi.org/10.1016/j.chemgeo.2021.120274.
- Will, T.M., Zeh, A., Gerdes, A., Frimmel, H.E., Millar, I.L., Schmadicke, E., 2009. Palaeoproterozoic to Palaeozoic magmatic and metamorphic events in the Shackleton Range, East Antarctica: Constraints from zircon and monazite dating, and implications for the amalgamation of Gondwana. Precambr. Res. 172, 25-45.
- Willner, A.P., Gerdes, A., Massonne, H.J., 2008. History of crustal growth and recycling at the Pacific convergent margin of South America at latitudes 29°–36°S revealed by a U-Pb and Lu-Hf isotope study of detrital zircon from late Paleozoic accretionary systems. Chem. Geol. 253, 114–129. https://doi.org/10.1016/j.chemgeo.2008.04.016.
- Willner, A.P., Massonne, H.J., Ring, U., Sudo, M., Thompson, S.N., 2012. P-T evolution and timing of a late Palaeozoic fore-arc system and its heterogeneous Mesozoic overprint in north-central Chile (latitudes 31–32°S). Geol. Mag. 149, 177–207. https://doi.org/10.1017/S0016756811000641.